



German-Dutch Wind Tunnels

# Annual Report 2006

Duits-Nederlandse Windtunnels

Deutsch-Niederländische Windkanäle





## **MAIL**

DNW  
P.O. Box 175  
8300 AD Emmeloord  
The Netherlands

## **E-MAIL**

[info@dnw.aero](mailto:info@dnw.aero)

## **WEB**

[www.dnw.aero](http://www.dnw.aero)

## **PHONE**

Exchange: +31 527 24 8555  
Central office: +31 527 24 8520

## **FAX**

+31 527 24 8582

The Foundation DNW has been established by Deutsches Zentrum für Luft- und Raumfahrt e.V. (DLR) and Stichting Nationaal Lucht- en Ruimtevaartlaboratorium (NLR).



# Contents

Preface	3
Occupation of Facilities – Status and Prospects	4
Highlights of Project Work	7
Fixed Wing Civil Transport Aircraft	7
Application of Pressure-Sensitive Paint (PSP) for Determination of Dynamic Surface Pressures on a Rotating 65° Delta Wing Model in Transonic Flow	7
Wind Tunnel Tests of a Transonic Natural Laminar Flow Wing	10
Military Aircraft	14
Dynamic Force Measurement on Two Transport Aircraft Configurations in the DNW-NWB	14
Investigations on a 1/7 Scale Advanced Hawkeye Model	17
JSF STOVL Testing in the LLF: A Review	20
The International Vortex Flow Experiment 2 in the DNW-TWG and the DNW-KKK	22
Environmental Engineering	25
The European Project MEXICO	25
Technical Status	27
Status of the Foundation	35
Publications and Presentations at Conferences	36
Organization of DNW	37



German-Dutch Wind Tunnels

# Preface

Reliability of operation of the wind tunnels becomes more significant in the course of increasing professionalization of aerodynamic testing and development. Whereas in the early days of the wind tunnels the tests were predominantly of exploratory nature and each researcher (group) needed a wind tunnel with easy and spontaneous access, at present the majority of tests is carefully planned beforehand by the “customers” for the test data allowing little spontaneity in the process. At times, the test teams coming to the wind tunnels have test programs defined by a number of different task groups at the home organization tied into one test entry needing to satisfy different requirements and stages of the development reducing flexibility to a negligible quantity.

These test programs, because of the interdependencies of the carriers of the test needs, require reliable test performances and time scheduling. In the experience of the operators of the wind tunnels in DNW, being able to hold schedules and being able to deliver the quantities of data with the quality beneficial to the customer has been one of the major characteristics motivating return customers from the global market. The challenge has been to provide the reliable service with an effort level that can be reasonably justified, and provide access without maintaining overcapacity.

A number of project highlights presented in the current annual report originate from non-European countries and bear witness to the capabilities of DNW on the global scale. The capabilities involved are not limited to the available infrastructure and instrumentation, but also involve DNW’s ability to interact with the customers and provide support on a level where the available skills are obviously needed and appreciated.

Despite the worldwide scope of DNW activities, without being embedded in the European network

of aerodynamic activities, and without the technological support coming with this network, any wind tunnel organization of this scope would be too weak to tackle the challenges lying ahead. Compared with the renewed effort going into wind tunnels as critical enabling technology in some other countries, more support should be available in our own supporting structure of home countries and European Community.

Considering the challenges facing the aeronautics industry worldwide, and considering the European ambition to be among those who shape the future, more investment than what is described in the examples in this Annual Report is needed. The investment into capabilities will benefit the society as a whole by guaranteeing tomorrow’s mobility with reduced environmental impact. Increased quality of testing is required for increased attention to the environmental consequences of flying. DNW considers the improvements in the technical status as described in the following chapters a good start into the future, nevertheless only a start.

By continuing its endeavor to combine high-technology testing with reliable systems that enable reliable test planning, DNW is simultaneously paying attention to two important requirements: the professionalization of wind tunnel testing and the need for scientific exploration for the benefit of the public at large. The chosen path requires careful balancing of priorities considering the finite scope of available resources. DNW hopes that this report documents a good balance, and that the first 25 years of successful cooperation with the European “star” Airbus, celebrated at the end of the year, will be continued with further successes in which the customers consider DNW a crucial part of the success.



## Occupation of Facilities - Status and Prospects

The year 2006 was another extremely busy year for DNW, and again predominantly due to the high work load in the LLF. As in the previous year, this annual report presents a number of highlights worth reporting. The most significant projects are reported in the chapter "Highlights of Project Work". The current overview presents a number of general observations, including the repeated occurrence of the non-uniform occupational patterns across the entire range of capabilities offered by DNW.

The biggest and perhaps also most challenging project in DNW tunnels continued to be the test entries for Airbus A400M propeller aircraft. The contents of this project have been reported in the previous years, and although it remains a highlight and continues to provide for a large part of the occupation of the LLF, the reader is referred to the Annual Report 2004 for more details. Based on the strength of this significant project of simulating pro-

PELLER effects in a fixed wing aircraft development, and the experience and know-how demonstrated by DNW in this project, the tests for the US propeller aircraft Hawkeye followed. Both the isolated propeller tests in the LST as well as the full model tests in the LLF are reported as highlights in the present annual report.

Another continuing large-scale project that was performed in the LLF was the development of the Lockheed Martin F35 aircraft, also known as JSF. DNW provided testing both for the jet effects in the STOVL configuration as well as for the inlet performance characteristics in the CTOL and STOVL configurations. Since this program came to its conclusion in 2006, at least as far as the aerodynamic development of the aircraft in wind tunnels was concerned, it is summarized as a highlight not only for one year in this report. This project has provided a significant contribution to the stability of occupation of the largest wind tunnel of DNW, the LLF,

and this stability will be missed in the coming years.

In previous years, the significance of testing for civil transport aircraft developments was smaller than that of the military market, especially for the industrial scale wind tunnels. This trend has continued, although the differences were not as pronounced as in the previous year. The LLF tunnel was an exception to this trend due to the EU-sponsored research activities for tilt rotor aircraft (Figure 1). In the HST the emerging regional jet development from China, the ARJ21 (Figure 2) and some other foreign passenger jet development programs provided some civil transport work as well.

As in the previous year, ground-based vehicle testing provided some exciting variation to the general testing activities. Whereas truck testing was a component in 2005, train testing provided a number of high-visibility alternatives to aircraft testing in 2006. Both the HDG and the KKK are well on their way to being accepted by the rail vehicle industry as important tools in the total development chain. In addition to low aerodynamic drag, high-speed trains also need low side wind sensitivity and high aerodynamic stability.

Another significant and highly visible area of expertise in DNW is the portfolio of testing services for dynamic phenomena. NWB continued the use of its Model Positioning Mechanism (MPM), providing unique maneuver simulation capability both for development and for research customers. This capacity, which was developed with the support of DLR research, has now reached a level of maturity that makes it an indispensable tool for industrial developments.

For the high-speed flight industrial domain as a whole, the year 2006 was a step in the right direction from the previous year. The organizational and technical changes in the HST have started to bear fruit, and the market response has been positive. A number of ongoing projects in the civil transport category could be provided with transonic test capability, for example the Piaggio project in the current report.

As in the previous year, a considerable share of the demand for high speed tests was provided by missile developments. This technology provided for a significant proportion of tests in the TWG. Another strong feature of the TWG is its usefulness for tests concerned with phenomenological research. Its price, flow quality and turnaround times make it ideally suited for exploratory work, such as the International Vortex Flow Experiment initiated in the framework of GARTEUR.

The range of capabilities in DNW ensures that



Figure 1: Tilt rotor model of the EU project ADYN in the 6 m x 6 m test section of the LLF

weaknesses in one market segment can be compensated by the strength in another, if the market develops at different rates in different segments. During the last few years DNW's operations owed their success to the strength in low-speed testing, primarily coupled with the simulation of ground effects for both fixed wing transport aircraft configurations as well as fighter configurations. The capability of simulating engine integration effects in ground proximity is expected to continue providing the bulk of testing volume into the following year, but not at the same intensity anymore. There are no large new fighter aircraft programs on the horizon. Also, since the largest industrial tunnel of the DNW, the LLF, obtains most of its high-intensity tests in the later phases of a development program, the new post-A380 projects will start appearing in the DNW planning with a few years delay.

Newly emerging aircraft development programs from countries such as China are expected to make use of the established strengths of DNW and will contribute to the occupancy of the industrial tunnels LLF and HST. The ARJ21 program has already made use of the HST.

The research market can be expected to remain stable, providing occupancy mainly in the smaller tunnels operated by DNW. The large EU-sponsored research programs still largely bypass DNW, as the priority seems to remain in establishing and supporting the capability provided by ETW. The exception to this trend is formed by the rotary wing air-

craft community including tilt-rotor aircraft. This community has no alternative for the scale advantages provided by the two large European wind tunnels, the DNW-LLF for low speed and the S1 of ONERA-GMT for high-speed testing, so a regular stream of moderate intensity will continue.

The US is the major non-European market for DNW's services. In this context the JSF has already been mentioned, the testing for Hawkeye under contract to US Naval Air Command as well. These two references bear witness to the quality of DNW's facilities and team, and they provide a basis for further activities in this market. On the other hand, in a number of studies performed for the US defense agencies, DNW has been identified as a major competitor, even as a threat to the national facilities. This has triggered funding for extra government support for NASA-operated facilities. It is still unclear, how this affects the amount of work DNW is able to attract from the US.

Overall, on the background of past experience and the developments in the aerospace world, the following year (2007) can be anticipated to be a year with fewer large industrial development projects than in the years past for the DNW as a whole. At the same time, this development will permit the planning for the urgently required maintenance and upgrading activities which have suffered in their priority in the last years of maximum tunnel utilization. Together with the response mechanisms in resource allocation in DNW in reaction to outside developments, DNW will be in a good position and continue to provide all the services the customers are used to expect from DNW.

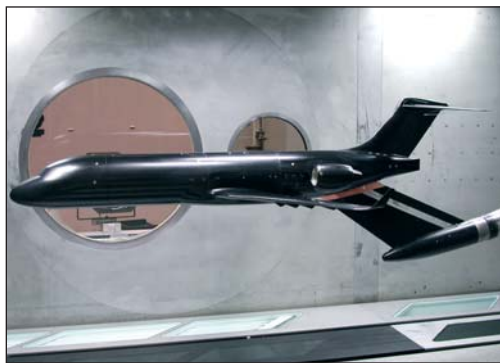


*Figure 2: Model of the regional aircraft ARJ21 of the Chinese FAI AVIC 1 in the HST*





## Highlights of Project Work

### Fixed Wing Civil Transport Aircraft

#### Application of Pressure-Sensitive Paint (PSP) for Determination of Dynamic Surface Pressures on a Rotating 65° Delta Wing Model in Transonic Flow

Becoming interested by the pressure data measured with PSP for steady cases the aerodynamicists working in the high-speed regime have been asking for a similar technique for investigations of unsteady flow phenomena, such as aeroelastic investigations, turbomachinery and helicopter rotors. This is the reason why DLR started an internal "Unsteady PSP" project in 2005, running until 2008, to develop the required hard- and software for industrial unsteady PSP measurements with a time resolution of better than 1 millisecond and with a sampling rate of up to 100 Hz.

Application of the PSP technique to unsteady aerodynamic flows requires special measurement instrumentation. The main challenges to obtaining acceptable PSP results are the development of hardware components, model illumination, and camera observation as well as the pressure-sensitive paint itself. First of all, a dedicated fast paint has to be designed as pressure sensor in order to reduce the response time of the paint with respect to pressure changes. DLR has developed a high porosity paint in which the luminescent dyes are incorporated in a porous polymer. Then, the instrumentation has to be able to acquire images with high framing rates and at low light intensities. Moreover, the software should be able to manage all the necessary synchronization between the PSP system and the wind tunnel in a short time.

The industrial aspects of the development will be considered in the DLR project as well, which means that the knowledge obtained from the implementation of these measurement techniques for industri-

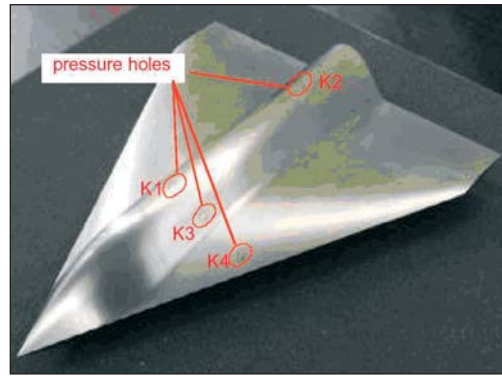


Figure 1: Delta wing model showing four pressure taps for comparison with PSP

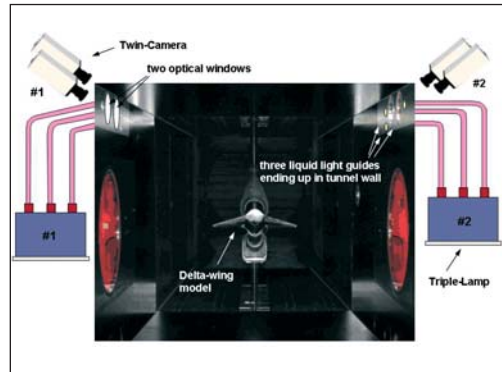


Figure 2: Test setup in the TWG; the painted model surface is illuminated from two sides

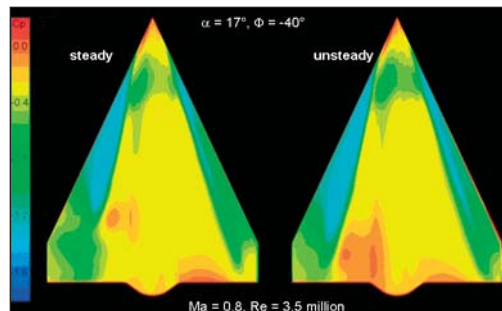


Figure 3: Steady and unsteady PSP data showing well-developed leading edge vortices

al wind tunnels will be used to develop a PSP system that is mobile and fast in both implementation and data processing.

The unsteady PSP measurements presented here are the first measurements that are part of this "Unsteady PSP" project carried out in the DNW-TWG in Göttingen. The investigated delta-wing model is made from steel with sharp leading edges. It has a length of 420 mm, a span of 333 mm, a leading edge sweep of 65° and a fuselage diameter of 60 mm, see Figure 1. On one side the model is equipped with four pressure taps (Kulite) which are used for comparison with PSP data. Therefore, they are operated in parallel to the PSP measurements. Only that model side which is equipped with pressure taps is painted with DLR's unsteady PSP formulation. The location of the pressure holes is also shown in Figure 1. The delta-wing model is mounted on a sting and the setup ensures a safe operation of the rotating model at a roll rate of up to 10 Hz.

All unsteady measurements presented here are performed at a constant roll rate of 10 Hz.

DLR has been developing pressure-sensitive paints in cooperation with a team from the Organic-Chemistry Institute of the University of Hohenheim. Since the unsteady pressure-sensitive paint should be usable on different model materials (e.g. carbon fibre, steel or aluminum) and should finally also be applicable to large and fully instrumented models, DLR has focused its efforts on pressure-sensitive paint formulations that can be applied by means of a spray gun. DLR has developed high porosity paints where the luminescent dyes can be incorporated into a highly porous polymer. The response time of the high porosity paint is about 1 ms and a total paint thickness of about  $10 \pm 2 \mu\text{m}$  was achieved. The drying time of this paint is about 10 minutes. The temperature sensitivity of the paint can be determined to be approximately  $-8 \text{ mbar}/^\circ\text{C}$ .

One high power UV flash light source is used for excitation of the paint ( $\lambda_{\text{ex}} = 375 \text{ nm}$ ) for each observation direction. Each light source consists of three separate high pressure Xenon bulbs with appropriate optical filters and each is connected to optical fibers of 2.0 m length. This means that a total of six fiber optics illuminated the painted model surface from two directions as shown in Figure 2. For each flashbulb up to 1 J white light in a  $100 \mu\text{s}$  pulse, equivalent to 10 kW peak power, was measured at the exit of each light fiber. A maximum repetition frequency of 0.2 Hz was attained for the high power flashes. The housing for the light sources is built to withstand low pressures in the plenum of the wind tunnel. For each lamp housing a microcontroller monitors the current run parameters (e.g. temperature, pressure and electrical capacity). It is connected with the PSP data acquisition system via the internal TCP/IP network. The maximum flash duration of the lamps is  $180 \mu\text{s}$ , depending on the actual power setting. A flash monitor output was used to determine the exact time of model illumination.

Cooled scientific CCD cameras with 14-bit resolution were used for image acquisition. A two-camera system for pressure and reference images is used to obtain the necessary images. Thus, pairs of images were acquired simultaneously by using the twin CCD camera system from each viewing position. With this arrangement, just one single flash of  $180 \mu\text{s}$  pulse length of the light sources is sufficient to provide a sufficiently large illumination for the CCD camera. That means that for a distance of about 0.5 m between the cameras and the PSP painted model, the CCD chip is exposed only once per frame by the luminescent light of the paint. Thus, the result represents the pressure distribution at a well defined time and no assumptions regarding

periodicity need to be made.

By using this experimental setup for investigations on the 10 Hz rolling delta wing, detailed information of the pressure distribution can be gathered by collecting individual images at different phase positions of the model.

As a result of the PSP measurement one obtains the pressure distribution on the model surface, which is delivered at each node of a structured 3D surface grid of the model. For calculation of absolute pressure values an in-situ calibration is added, which is determined by comparison of pressure tap values with the PSP results at the location of the corresponding pressure taps in the wind tunnel model. Data reduction using DLR's ToPas software is performed by scripting methods with a very high degree of automation and reproducibility.

For a roll angle  $\theta = 0^\circ$ , the model is in the horizontal position and the local angle of attack is maximum. For a roll angle  $\theta = -90^\circ$  the model is in the vertical position and the local angle of attack is  $0^\circ$ . At all the other phases during the roll of the model, there is a continuous variation between these two types of flow field.

Figure 3 shows a typical PSP result of the suction side of the investigated model, using the phase locked unsteady PSP data acquisition, for the steady and unsteady case, for  $Ma = 0.8$  and  $Re = 3.5$  million at an angle of incidence  $\alpha_{\text{NOMINAL}} = 17^\circ$  and a roll angle  $\theta = -40^\circ$ . For both cases well developed leading edge vortices can be seen in the PSP results. In the steady case vortex breakdown occurs on the port side of the wing. This can be seen in the PSP result from the strong pressure gradient. In the unsteady case the vortex breakdown on the port side of the wing is shifted downstream. With the newly developed unsteady pressure-sensitive paint formulation the dynamic behaviour of the complete surface flow becomes visible.

*Contributed by Christian Klein, Ulrich Henne, Werner Sachs, Yasuhiro Egami (all DLR), Vlado Ondrus, Uwe Beifuss (both University of Hohenheim)*

## Wind Tunnel Tests of a Transonic Natural Laminar Flow Wing

### Introduction

The design of a new Natural Laminar Flow (NLF) wing has been carried out recently at CIRA with the collaboration of Piaggio Aero Industries S.p.A., in the framework of the research project VITAS, funded by the Italian government. The new wing has two design points at  $Ma = 0.75$ ,  $C_L = 0.5$  and  $Ma = 0.78$ ,  $C_L = 0.46$ , both at  $Re = 8 \times 10^6$  (based on the mean aerodynamic chord), and it was designed to work with a natural laminar flow extension of up to 60% of the wing local chord.

In order to check the performance of the newly designed laminar wing, an extensive wind tunnel test campaign in the transonic regime at flight Reynolds numbers was performed on a 1:6 scaled half-wing model in the DNW-HST in January 2006 (Figure 1).

### Wind tunnel model and test set-up

The wing design refers to a medium size business jet whose weight and selected flying conditions require wing target performances extended over a wide spectrum of aerodynamic conditions (multi-point design). The wing is  $16^\circ$  tapered swept back with an aspect ratio of 8 and a taper ratio of 0.34. This configuration is a compromise between conflicting requirements, namely: low-speed flying qualities (long tip chord to limit the performance degradation deriving from the reduction of the Reynolds number), low induced drag (high aspect ratio) and structural aspects (thick root sections which require long chords in order to limit the compressibility at high speed). The wing is supposed to be mounted below the fuselage; a dihedral angle of 2 degrees was adopted.

The half-wing model has an exposed span of 1272.5 mm and a root chord of 535 mm. The model is made of one-piece machined main element, including an integrated mounting interface,

and is equipped with two cover panels located on the bottom side. Dedicated low thermal conductive panels are installed on the upper side, in order to permit the use of the infrared thermography technique. The overall span of the model, including the integrated mounting interface, is 1593 mm. The model was equipped with 129 pressure taps, located along two chord wise stations, at 30% and 70% of the full span. A total of five high frequency pressure transducers were also installed on the model, in order to measure the laminar, turbulent and separated boundary layer fluctuating pressure.

Forces and moments were measured with a five-component external pyramidal balance, installed on the test section sidewall. The model mounting interface is a big plate crossing the turntable, fixed between the two interface flanges of the balance located outside of the test section.

A proper fairing, not weighted by the sidewall balance, was used to move the model out of the test section wall boundary layer while shielding the wing interface with the sidewall balance without any fouling contact; its shape had to ensure that both the load distribution on the model was representative of that of the isolated half-wing (as this was developed and tested numerically) and the boundary layer on the wing surface was neither contaminated by that developed on the fairing (that can cause leading edge contamination) nor from air blowing from the plenum to the tunnel test section and vice versa.

### Test campaign

The test campaign was primarily aimed at the confirmation of the good design of the wing in terms of laminar flow characteristics. Selected tests were carried out to check the transition position on the upper side of the wing, using the infrared thermography technique. Natural laminar flow visualization was performed using two Thermovision A40M infrared cameras. The image resolution of both cameras was  $320 \times 240$  pixels. Special glass windows coated for IR measurements were mounted on the tunnel ceiling slats.

IR images were taken at assigned values of  $C_L$  for several Mach- and Reynolds numbers. The acquisition was performed at fixed angles of attack in order to reach temperature equilibrium on the model surface. Some seconds before the recording the cooler downstream of the fan was switched off in order to increase the air temperature and to consequently amplify the temperature difference with the wing surface and resulted in images with a very good resolution and rich details. As summarized in Table 1, the selected test conditions for the IR tests covered the design points of



Figure 1: The UW-5006-NLF wing and fuselage installed in the HST

the wing in terms of Mach number and  $C_L$ , but also investigated its behavior off-design, at  $Re = 4$  million and at  $Ma = 0.6$ .

Mach number	Reynolds number	$C_L$
0.75, 0.78	$4 \times 10^6$	0.4, 0.45, 0.50, 0.55
0.6, 0.7, 0.75, 0.78, 0.8	$8 \times 10^6$	0.4, 0.45, 0.50, 0.55
0.6, 0.7, 0.75, 0.78, 0.8	$10 \times 10^6$	0.4, 0.45, 0.50, 0.55

Table 1: IR tests

Force and pressure tests were carried out to measure the aerodynamic coefficients at Mach numbers between  $0.5 < Ma < 0.82$ , both with free transition at Reynolds numbers varying between  $4 \times 10^6$  and  $10 \times 10^6$  and fixed transition at  $Re = 8 \times 10^6$ . In addition, both the aerodynamic coefficients and the stall behavior were evaluated at low speeds with free transition in the range of Reynolds numbers between  $4 \times 10^6$  and  $10 \times 10^6$ . Where required, boundary layer transition fixing was achieved by means of mini dots at 5% of the local chord on the upper and lower surface.

Pressure distributions were acquired together with the load coefficients, along the two instrumented stations of the wing, respectively at 30% and 70% of the wing span, with three ESP modules installed inside the model with 15 psi full-scale, for a total of 129 pressure taps. A flow visualization test with oil and titanium dioxide was performed at  $Ma = 0.78$  at cruise condition. Finally, some additional measurements were performed during the test campaign such as visualizations of the stall pattern with mini tufts at  $Ma = 0.3$ ,  $Re = 4 \times 10^6$  and  $10 \times 10^6$ , unsteady pressure measurements with Kulite sensors within the laminar, turbulent and separated boundary layer, and wake pressure measurements.

## Test results

### Laminar flow assessment

Figure 2 shows the results of the flow visualization with oil and titanium dioxide (applied only on the outer part of the wing), carried out at  $Ma = 0.78$  and  $Re = 8$  million, together with an IR image taken under the same conditions.

The region where the flow is laminar appears colder than the turbulent region in the IR image. This is due to the lower heat transfer that occurs in laminar flow. In other words, the air which has a higher temperature than the wing warms the model up more in the turbulent than in the laminar region. In the pictures the laminar regions show a deep blue color, while the turbulent regions have a red or orange color. From the picture some turbulent

cones can be seen, probably due to some imperfections of the paint covering the wing surface. It can be stated that at  $Ma = 0.78$  a successful extension of natural laminar flow was obtained on the model upper surface up to 70% of the chord length. In the central and outer part of the wing, the laminar flow extends up to the shock wave position. The latter can be identified as straight lines with a red or orange color that extend along the wing span from 30% up to the tip. The triangular blue region near the root is not to be interpreted as a laminar region but as a flow of cold air coming from the gap between the wing and the fuselage. Probably this unexpected flow of air caused a disturbance near the root region that prematurely anticipated the transition.

The oil flow visualizations match very well with the IR images. It is interesting to note how the oil flow visualization has been able to discriminate between laminar and turbulent flow, even if this technique is not suitable for transition visualization. It can be noted that the extension of the laminar region is a little bit shorter on the oil flow image; this is due to the presence of the oil layer itself, whose convection towards the trailing edge wastes some of the kinetic energy of the boundary layer. The presence of a number of turbulent cones is instead due to some local titanium dioxide accumulations that are typical for this technique, that trigger the boundary layer transition.

If the boundary layer is laminar, a colder, blue region is visible on the IR image after the hot, red trace of shock wave. It is almost certainly due to a recirculation bubble that occurs under the wide lambda shock that locally increases the temperature as the flow speed is lowered. The bubble is followed by flow acceleration that is responsible for the small colder region after the shock wave line. The corresponding station on the oil visualization shows an

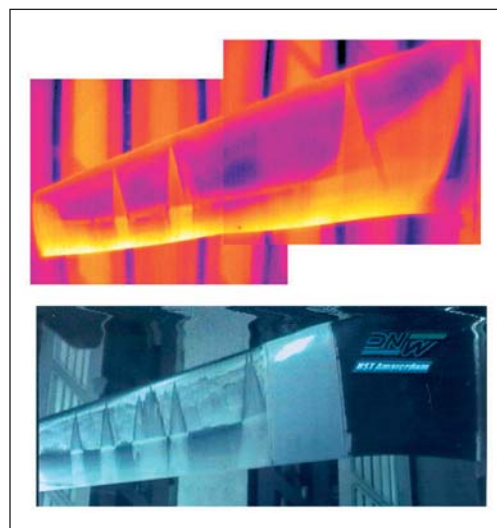


Figure 2: Comparison between IR and oil visualization at  $Re = 8 \times 10^6$ ,  $Ma = 0.78$ ,  $\alpha = 2.5^\circ$  and  $C_L = 0.55$

oil accumulation, followed by a clean surface. This is the effect of the recirculation bubble that entrains the oil towards the leading edge and therefore leaves a cleaner region just behind the shock wave location as the oil entrained towards the trailing edge behind the shock wave cannot be replaced by fresh oil coming from upstream.

If the boundary layer is turbulent, the interaction with the shock happens in a much shorter region, and the recirculation bubble does not occur as the turbulence increases the ability of the flow to remain attached. The temperature suddenly increases behind the shock wave, but this now happens closer to the model surface than in the laminar flow case, so without the buffer effect of the thicker boundary layer that forms after the recirculation bubble. The effects are clearly visible on the IR image that shows a step-like increase of the surface

temperature. The corresponding station on the oil flow visualization shows a similar clear boundary between the laminar and turbulent regions. This is due to the sudden deceleration of the flow that reduces the oil entrainment and to the abrupt pressure rise that causes a barrier-effect to the liquid film both resulting in a gradual accumulation of the oil in front of the shock wave line. In the following region the oil entrainment is lower and the part that is swept away by the flow is replaced by the upcoming flow, therefore resulting in the neat white region shown in the picture.

### Forces and moments

The main scope of the test campaign was the confirmation of the laminar design of the wing through IR visualizations. Nevertheless, forces and moments were acquired on both the free transition and the fixed transition (5% of the chord) configurations, in order to characterize the wing aerodynamics and to appreciate the benefits of the laminar design of the wing in transonic regime.

Figure 3 shows the effect of a Reynolds number variation as well as the effect of fixing the boundary layer transition on the lift coefficient at the cruise Mach number  $Ma = 0.78$ . The Reynolds number effect in the presence of a natural laminar flow on the wing is very small (between  $Re = 8$  and  $10$  million), and is limited to high angle of attacks. At  $Re = 10$  million, buffet phenomena and non-linearity occurred at a lower angle of attack with respect to  $Re = 8$  million. With the transition fixed,  $\alpha_{CL}$  increases with respect to the free transition tests, even of the order of 1 degree in the transonic regime, whereas the lift slope does not change appreciably. The global effect is a reduction of the lift at all model attitudes up to stall. This is confirmed by the pressure distribution (Figure 4). The shock position moves forward when the transition is fixed.

The most important effects are visible on the wing polar (Figure 5). This wing has a  $CD_0$  of about 80 to 90 drag counts at the design condition, and with a fixed transition at 5% of the chord on both the upper and lower surfaces, the wing drag increases by about 30 counts at the same Reynolds number and lift condition. Note also the slight improvement at  $Re = 10$  million with respect to 8 million at low lift coefficient that is probably due to a more extended natural laminar flow region in the first case. On the contrary, at the cruise  $C_L$  the results at these two Reynolds numbers are coincident as confirmed by the IR images.

Figure 3: Reynolds and transition fixing effects on the lift curve at  $Ma = 0.78$

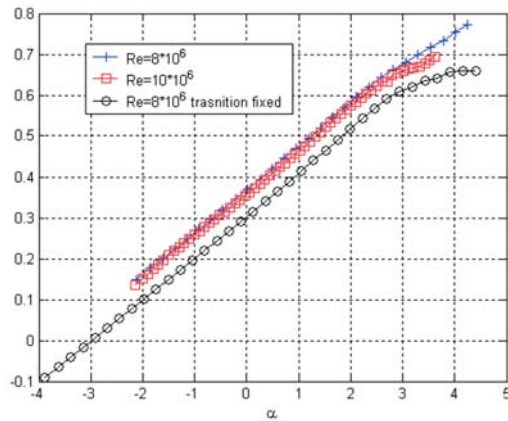


Figure 4: Comparison of shock position between free (\*) and fixed (o) transition cases;  $\alpha = 2^\circ$ ,  $Ma = 0.78$ ,  $y/b = 70\%$

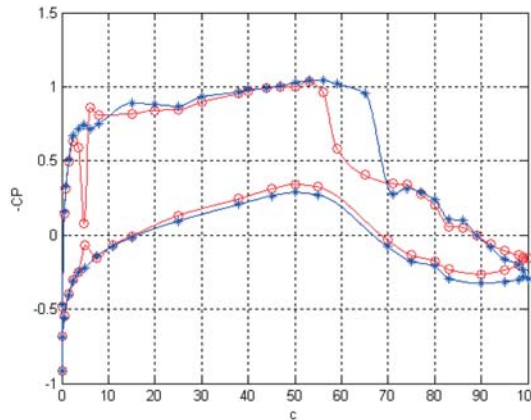
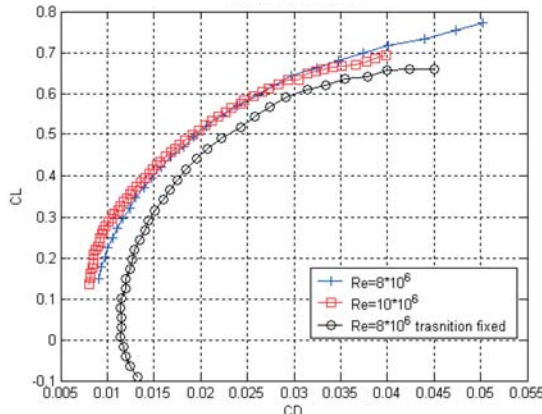


Figure 5: Reynolds and transition fixing effects on the drag at  $Ma = 0.78$



### Conclusions

A successful wind tunnel test campaign has been carried out on a new experimental transonic wing

designed to achieve natural laminar flow. Wind tunnel test results were presented, showing the capability of the NLF wing to confirm the performance predicted during its design. In fact, the results showed the achievability of a wide region of laminar flow in the transonic regime up to 60 – 70% of the wing local chord at design conditions.

The solutions adopted to resolve the challenge in the wind tunnel model worked well, avoiding both leading edge contamination caused by the wind tunnel wall boundary layer and leakage through the labyrinth. Nevertheless, during the tests an unexpected air flow was observed at the wing root due to the particular fuselage cavity design. This was however rapidly solved during the tests that were completed successfully.

*Contributed by Piaggio*



## Highlights of project work

### Military Aircraft

#### Dynamic Force Measurement on two Transport Aircraft Configurations in the DNW-NWB

##### Introduction

The NWB has performed dynamic force measurements for Airbus for almost a decade. The measurements were aimed at determining dynamic derivatives and have been performed with great success.

Methods and testing infrastructure have both improved regularly during this period. Starting with the Mobile Oscillatory Derivative balance MOD, which was developed during the seventies, and continuing with a hydraulic parallel kinematic platform (Hexapod), the NWB currently uses the unique Model Positioning Mechanism (MPM) for the dynamic wind tunnel tests.

##### Objectives

The test campaign DYNDER was established for two different reasons: firstly, to prove that the changes in the test setup provide consistent results and secondly, to determine the differences in dynamic derivatives resulting from two different transport aircraft models tested very recently.

##### Model and test set-up

Two different wind tunnel models were used, i.e. the models DYNDER 17.2 and DYNDER 17.3, which represent different development statuses of a transport aircraft. The DYNDER 17.2 model was tested extensively in the NWB in 2003, while the DYNDER 17.3 model was built in 2006 especially for the DYNDER test campaign.

Both models feature characteristics that are typical for dynamic testing models: extremely lightweight, but stiff CRP sandwich construction, modular



design, and options for monostrut and three-strut mounting.

The monostrut support was used together with an internal six-component strain gauge balance, while the three-strut support was used in the unique three-part, six-component piezo balance of NWB. Static, as well as dynamic model positioning (for monostrut and three-strut mounting) was performed with the MPM.

The MPM, as shown in Figure 1 with a generic transport aircraft, is a motion platform with six degrees of freedom, implemented as a parallel kinematic system. It consists of a movable platform that is linked to the wind tunnel fixed base by six constant length legs. These legs are joined with the platform as well as with six carriages that can move along two parallel guiding rails. The six carriages are equipped with electric linear motors and run independently of each other.

Similarly to the previously used hydraulic system, an additional actuator is installed. This actuator is used to generate sinusoidal high-frequency pitching and rolling oscillations. This seventh actuator is also an electric motor and is controlled by the same Sinumerik control system as the other six axes of the MPM system.

The advantages of the MPM with respect to its predecessors include the quality of the model oscillations and the high eigenfrequencies of the system resulting from the stiffness.

### Test program

The test program consisted of three wind tunnel entries in 2006. The first entry, using the 17.2 wind tunnel model, was used to compare the results of static and dynamic measurements with the results obtained from campaigns that were carried out in 2003 with the same model.

In the second wind tunnel entry, static and dynamic measurements were performed on the DYNDER 17.3 model on MPM and ventral sting, as shown in Figure 2. The dynamic measurements were performed in the modes pitch, roll, yaw, plunge (= heave) and lateral oscillation.

During the third campaign, the DYNDER 17.3 model was mounted on the unique three-strut support of the NWB to perform static tests, as well as dynamic measurements in the yawing motion. This setup is shown in Figure 3.

### Results

The improvement in the quality of the oscillatory motion is indicated by the frequency spectrum of the signals of the internal six-component strain gauge balance, as the wind-off balance signals are proportional to the acceleration in the corresponding direction.

The time-dependent signals and the corresponding

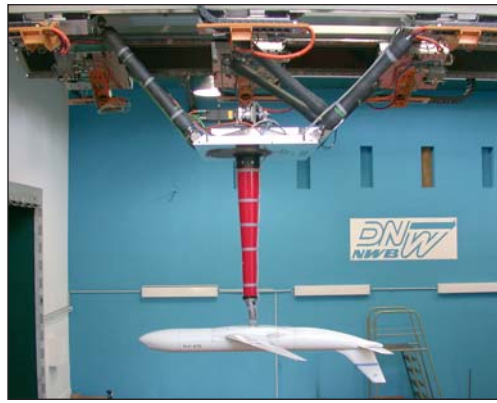


Figure 1: NWB's model positioning mechanism MPM

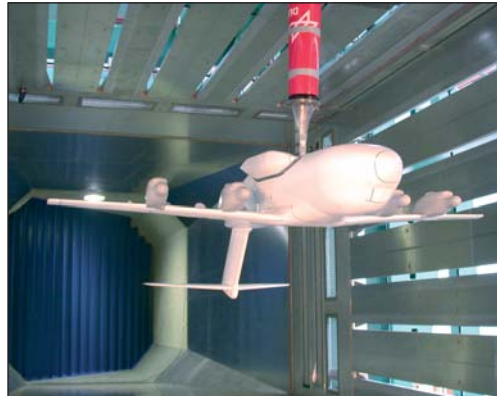


Figure 2: DYNDER 17.3 model on a ventral strut in the NWB

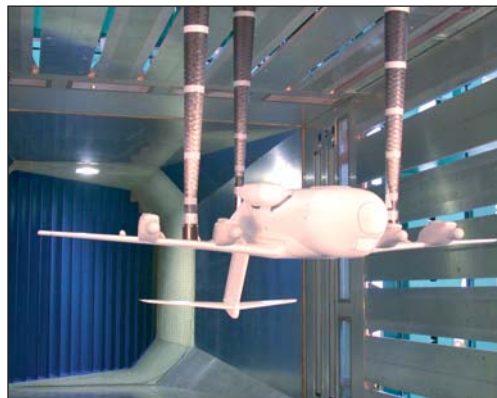


Figure 3: DYNDER 17.3 model on a tristrut support in the NWB

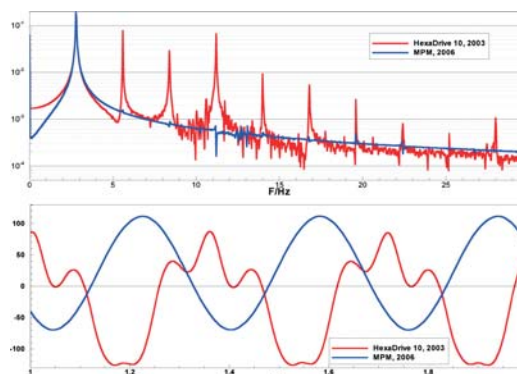


Figure 4: Time signal and frequency spectrum of the pitching moment

frequency spectra of the pitching moment signal as shown in Figure 4 clearly indicate the reduction of higher harmonic components in the MPM's motion as compared to the motion generated by the Hexapod system.

Figure 5: Lift, drag and pitching moment coefficients of the DYNDER 17.3 configuration in upright and inverted mounting position

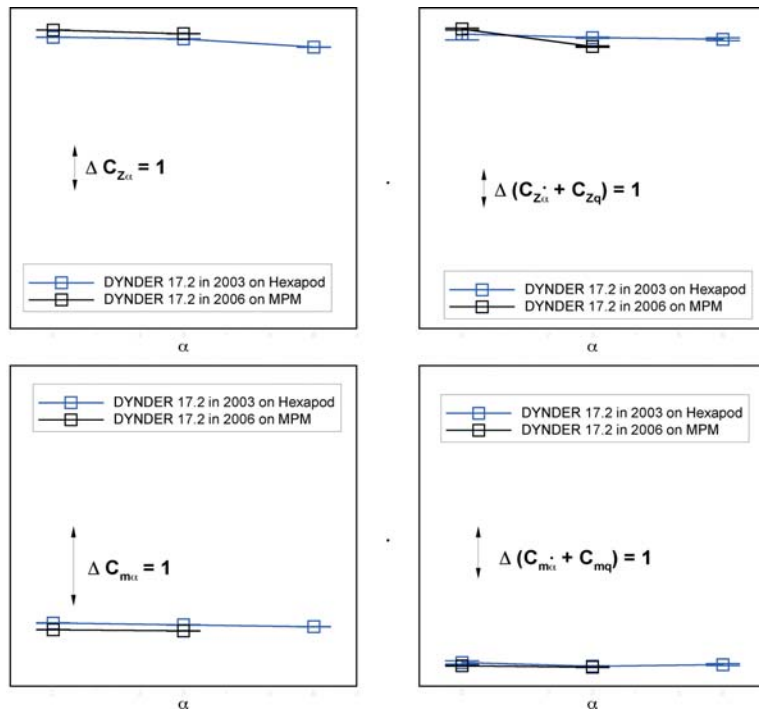
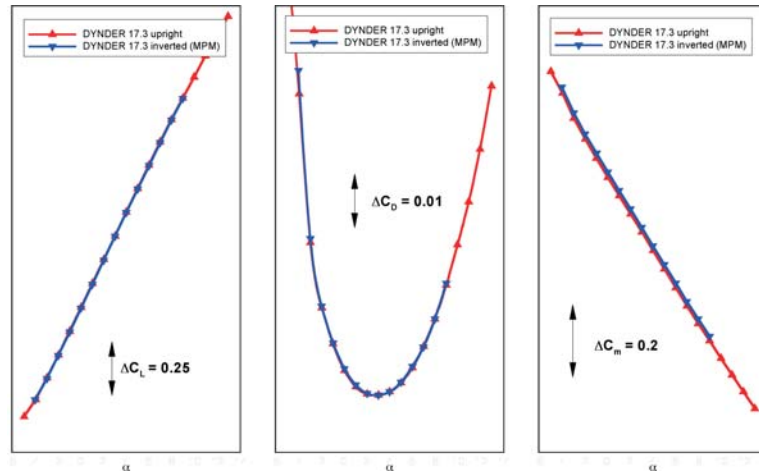


Figure 6: Dynamic derivatives of the pitching motion; comparison between results from 2003 on the Hexapod and 2006 on the MPM

Examples of the static measurements lift, drag and pitching moment coefficients of the DYNDER 17.3 configuration are given for an upright, as well as an inverted mounting position (Figure 5). The agreement is very good for the pitching moment and excellent for lift and drag.

The dynamic derivatives calculated from the pitching motion are given in Figure 6 and serve as an example of the dynamic measurements. In general, the agreement is very good; the differences are of the order of the line thickness. The small differences may be attributed to the more precise oscillations of the MPM. The DYNDER 17.3 results of the yawing motion on the three-strut support show a closer match to the corresponding results on the monostrut support than was the case in previous cam-

paigns. The reason for the closer match can be essentially attributed to improvements in the data evaluation software. However, the more accurate movement of the model by using the new MPM also contributes to a closer agreement.

### Summary

The three DYNDER test campaigns were accomplished with great success. The MPM was established as Hexapod's highly improved successor; with consistent results of static and dynamic measurements. The results of the three-strut measurements confirm the corresponding values of the monostrut measurements.

## Investigations on a 1/7 Scale Advanced Hawkeye Model

The E-2 Hawkeye is the US Navy's all-weather carrier-based early warning, command and control aircraft. The E-2 is a twin engine, high-wing turboprop aircraft with a 7.3 m diameter radar rotodome attached to the fuselage. The aircraft can track numerous targets simultaneously and can direct numerous intercepting aircraft at the same time. With their highly advanced antennae, radar and communications systems, these aircraft are called the "eyes of the fleet". The current version of the E-2C aircraft has undergone several upgrades to its sensors, engines and propellers. The newest running variant of the E-2C (Hawkeye 2000) is supplied with a new mission computer, improved radar displays and Cooperative Engagement Capability. The model tested at the DNW-LLF will be the next generation: the E-2D Advanced Hawkeye which is currently in development, using the E-2C Hawkeye 2000 as a baseline configuration. The maiden flight of the Advanced Hawkeye is scheduled to take place in August 2007. The plans are to introduce the new airplane to the fleet in 2011.

In view of the strict stability and control requirements and the unusual shape of the aircraft in combination with powerful turboprops, extensive wind tunnel tests were started in 2006. A 1/7 scale wind tunnel model was designed and built by NLR. The work was commissioned by Northrop Grumman in close cooperation with Naval Air Systems Command (NAVAIR). The test objective of NAVAIR was to conduct high-fidelity wind tunnel tests with two different powered propeller configurations. The results of the wind tunnel tests will help in achieving improvements in the behavior of the stability and control qualities, as well as simulations of power effects of the propellers. Moreover, the results will help in investigating the aerodynamic performance of the airplane – especially loads on the wings and the tail section – and in creating a high-fidelity aero-database to support the maiden flight of the Advanced Hawkeye. This is why the model was primarily designed for investigations of performance and control characteristics in the LLF 8 m x 6 m and the 6 m x 6 m test sections (Figure 1).

The model has a length of 2.5 m and a wing span of 3.5 m. The high-lift model is constructed of aluminum, steel and composite material. The model's support system in the wind tunnel can either be a ventral or a dorsal sting arrangement. The ventral setup was used for testing in cruise flight conditions. The dorsal setup will be used for investigations of ground proximity effects that are needed to simulate take-off and landing conditions. The stings are not only used to hold the model in the tunnel



Figure 1: Model of the Advanced Hawkeye in the 8 m x 6 m test section of the LLF

but also as a duct for the instrumentation cabling, as well as for the supply and return lines of the compressed drive air for the motors.

The fuselage of the model is equipped with a new, six-component internal balance for measurements of the overall model forces and moments, consisting of aerodynamic contributions and propeller thrust. This balance was built especially for the Advanced Hawkeye model. Each of the two propellers of the plane is driven by motors that are running with compressed air. The motor nacelles are mounted under the wings. The mounting system of the nacelles can be tilted in order to enable simulations of the thrust tilt. To reach the needed performance, the required maximum compressed air pressure is about 75 bar directly at the motor inlet. In order to prevent icing conditions at the exhaust, the drive air coming from the DNW air distribution system is pre-heated up to 65°C. The air consumption to run at nominal rotational speed of 7740 rpm is dependent on the applied blade pitch angle at the propeller. The maximum air consumption is about 2.5 kg/s per motor. The drive air for the compressed air-driven motors is guided via air pipes through the model support into the fuselage, across the internal main balance and the wing to the motors. To ensure proper simulation of the interaction between the propeller slipstream and the wing, and/or interaction between the tail section and the elevators and rudders, the expanded cold turbine flow is not exhausted through the motor nacelle. Instead the exhaust air is guided back via the wing and fuselage structure, across the balance and the model support, and is exhausted behind the model through two mufflers mounted on the torpedo (see the blue support structure in the background of Figure 1). In order to minimize parasitic effects to the internal balance caused by ducting the high pressure mass flow across the balance, a new two-way bridging system was developed and mounted in the airline (Figure 2). These air-line crossovers – also called airline bridges – are used for the high-pressure supply air as well as the low-pressure

Figure 2: Airline bridges for the reduction of parasitic effects to the internal force and moment balance



Figure 3: Schematic of the propellers

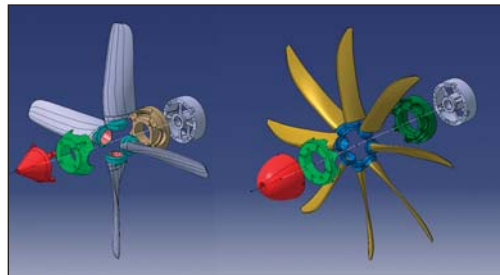


Figure 4: Impression of the complexity of instrumentation inside a wind tunnel model



Figure 5: Remote control unit for the elevators

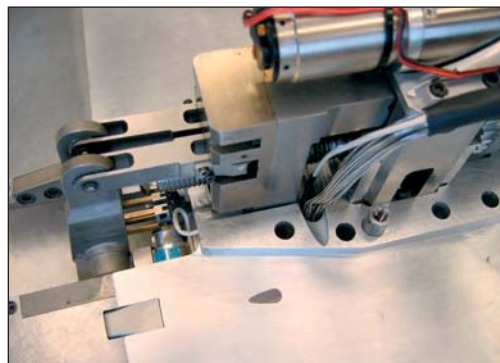


Figure 6: Set-up of the isolated propeller test in the LST; the insert shows a rotating shaft balances



return air (which is still above 10 bar) to and from the turbines of the air motors.

Two propeller sets for the conventional four-bladed propeller and for the new NP2000 eight-bladed propeller are available for each motor. This allows preparations of one propeller set while the tests are being performed with the other set. All the eight propellers are manufactured of carbon fiber material. The propeller forces and moments are measured with two six-component Rotating Shaft Balances (RSBs) that are mounted in between the propellers and the drive motors. Figure 3 shows a sketch of both propeller types and the RSB. For each RSB the data was transmitted via a slip ring set to be acquired and processed by the dynamic data acquisition system of the LLF.

The model (Figure 4) is equipped with approximately 300 steady pressure taps at the fuselage, the wings and the tail section. This allows local pressure profiles and steady loading to be determined. In addition, pressure sensors are applied at the scoops and the nacelles. The pressures are measured simultaneously with an electronic pressure measurement system based on a Scanivalve RAD system.

The elevators of the model are both driven by a specific linear actuator located under the stabilizer. An actuating lever is fixed at each elevator root, and each lever is connected to the sliding part of the actuator by means of a rod (Figure 5).

Prior to the first powered Hawkeye tests performed in the LLF, DNW carried out tests for the propeller/RSB combination in the 3 m x 2.25 m test section of the LST (Figure 6). This so-called isolated propeller test utilized an existing rig consisting of a streamlined vertical strut and a horizontally mounted nacelle. The nacelle is designed to mount all the drive train components as they are used also in the LLF-model (propeller including spinner and hub, RSB, torque meter, slip ring and the air motor to drive the propeller). The behavior and performance of all the propellers, RSBs, slip rings and air motors were tested for several operational conditions. The test rig for the isolated propeller test was also used to verify the calibration matrices of the RSBs. Until then, these matrices had been derived in a static dead weight calibration set-up. This is the reason why the propeller was replaced by calibration tools enabling the application of weight loads while turning the engine axis and the RSB.

The first test at the LLF was performed in the 6 m x 6 m test section. The model was mounted in the ventral set-up arrangement. The wind tunnel speed ranged from 44 m/s up to 134 m/s for the simulation of cruise-flight conditions. The tests assessed and compared the in-flight aircraft performance and stability for the two different propeller designs. The major part of the tests, however, focused on

the new NP2000 eight-bladed propellers of the E-2D Advanced Hawkeye.

In order to determine the support interference effects for use as correction data of the measurements with the dorsal or the ventral sting configuration, a mirror dummy support was constructed for the second Hawkeye test in the LLF. This second test started in December 2006 and is scheduled until mid February 2007. Due to the complex model geometry, especially the rotodome above the fuselage and its aerodynamic interaction with the tail section, interference testing is more complicated than is the case for usual airplane configurations. The dummy support is used to test a series of eight different support arrangements. The support corrections for the dorsal and ventral sting measurements are evaluated by combining the aerodynamic coefficients of the eight relevant configurations within the complete envelope for angle of incidence and angle of yaw. The resulting data is stored in a database and is available for online corrections of future measurement campaigns.

In addition to sting interference, the second Hawkeye wind tunnel test in the LLF concentrates on creating an out-of-ground database.

A third wind tunnel test is planned for 2007 in order to build up a database for in-ground effects. By implementing the LLF's moving-belt ground plane and sucking off the incoming boundary layer flow of the wind tunnel, a simulation of take-off and landing configurations with all the necessary high-lift devices will be performed.

## JSF STOVL Testing in the LLF: A Review

Within the last decade, the testing for the JSF project was one of the most significant activities for all of DNW. This testing provided both a heavy rate of occupation as well as a steady drive for improving the operational productivity of the LLF. In addition to the operational productivity increases achieved by DNW's continuous improvement activities a number of firsts were also achieved within the JSF testing sequence. Although a number of these activities have been reported in previous annual reports, it seems appropriate to pass review now, after the last tests in both the STOVL jet effect series as well as inlet tests have been completed (in 2006 and 2005 respectively). From now on the experience obtained on the DNW side in the relevant experimental simulation will have to wait until the flight tests provide more information about the aircraft behavior in full scale.

The testing in DNW for the JSF program started before either of the two significant decisions were made: the decision to participate in the project by the Dutch government and the decision by the US government to award the contract to LM Aero Company. In the early phases both the HST under contract to Boeing, as well as the LLF under contract to LM Aero were involved in the testing. After the decision by the US authorities to continue with the LM Proposal for JSF, only the LLF has been involved in the testing.

For the STOVL jet effects a total of 13 test entries with several models was performed in the LLF. The 12 % scale models were provided by the customer LM Aero. The first two test entries, in 1998, were performed in the concept demonstration phase in a novel technical setup for DNW. The model was smaller than is the case in the more standard testing for civil transport aircraft, and the compressed air requirement for controlled supply of the jet mass flow rate of up to 8 kg/s continuously was larger

than usual up to that time. To the satisfaction of the LM team, all the targets were reached, and the average simulation productivity in the wind tunnel was almost 50 polars/day (48 and 47 polars/day respectively in the first test entries).

For the continuation of the testing and as part of the technology team assembled by LM Aero JSF project, DNW had to continue to improve its productivity and also the compressed air supply system. In fact, the availability of precisely controlled air was a critical prerequisite for achieving high productivity. The DNW compressed air system is capable of supplying about 6 kg/s continuously, although temporarily about 12 kg/s can be delivered. In order to reach continuous compressed air supply of up to 8 kg/s, the air supply lines of DNW were augmented by a liquid nitrogen evaporation plant rented from an external supplier. This solution enabled DNW to reach the required mass flow rate without tying up all of its investment capacity in this one project of increasing compressed air supply. At the model end of the compressed air provision system, four air lines were providing separate air flows to the lift fan, the core engine and the two roll nozzles. In each line two control valve units were incorporated; one for the coarse and the other one for the fine control of mass flow rate. Per nozzle the control precision achieved was  $\pm 10$  g/s at a supply of 3 kg/s per nozzle. Other technical achievements can be found in the Annual Report of 2002.

With all the improvements in the speed of control, technological capabilities and skills of the team, the total productivity was increased to 80 polars/day on the average, and practically doubled in the year 2005, when in the test entry SJ-05 an average of 100 polars/day was achieved. This, since the polar rate is also dependent upon the number of (manual) configuration changes required, and in that entry the configuration was not changed frequently.

Another innovation introduced in the course of testing for the JSF jet effects was application of the DNW Particle Image Velocimetry (PIV) in a flow field where high and low speed effects were present simultaneously, see Figure 1. An internal development project preceded the test, where both the compressed air in the air delivery lines to the core nozzle and the lift fan (at pressure level of about 15 bar) as well as the free stream flow of the LLF had to be seeded with particles detectable by the PIV system. (The PIV system of DNW itself has been described in previous annual reports). The quality of results obtained in the course of a capability demonstration test exceeded the expectation and the available data from the first try was sufficient for the needs of the project.

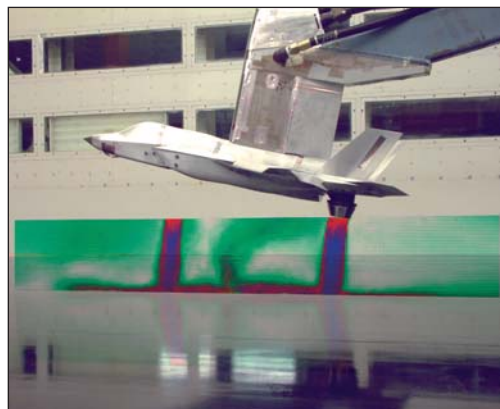


Figure 1: JSF STOVL model including graphical presentation of PIV measurements in the LLF

In addition to the jet effect test series also the JSF engine inlet flow conditions were measured in two extensive test entries, see Figure 2. For this, another novel type of testing for DNW, a major investment into suction capability, funded by the customer, had to be completed at short notice. A number of options for providing the inlet suction capacity were considered; the final choice was to install eight vacuum pumps of the roots blower type, each with a capacity of 3.5 kg/s at atmospheric pressure. The roots blowers had to be individually calibrated in order to achieve the required accuracy in inlet mass flow measurement.

A model scale of 20% was chosen in order to accommodate all the required instrumentation in the fan and core inlet ducts, and on the lift fan door and auxiliary inlet doors. For data acquisition from the 460 steady state pressure ports and 144 high response pressure sensor ports both the DNW standard data acquisition system as well as the Dynamic Data Acquisition (DDA) system were successfully applied, see Figure 3. In particular the DDA system, a DNW proprietary development, proved its value in these tests. More information can be found in the Annual Report of 2004.

Although the year 2006 saw the last development test for the LM Aero JSF project, the effect of participating in such a project from the early stages up to the start of the flight testing will last in terms of increased capabilities and know-how. The effect of having worked as part of an international team (as is the rule rather than the exception for DNW) and having mastered specific novel challenges in close cooperation with the LM team has again proven the versatility and adaptability of the DNW team. The tests were not only among the highlights of the year 2006, but also of a whole period. DNW looks forward to complementary tests in the further cycles of the product improvements.

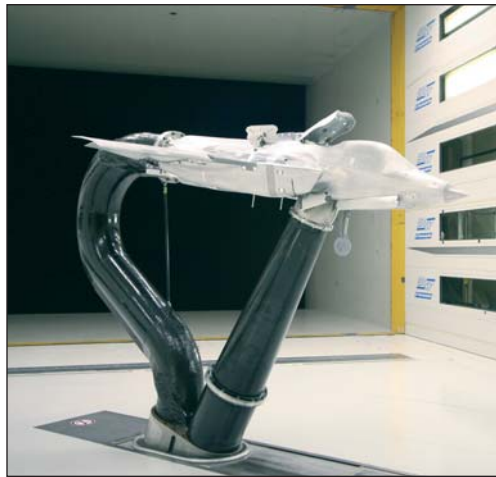


Figure 2: JSF inlet model on roots blowers in the LLF

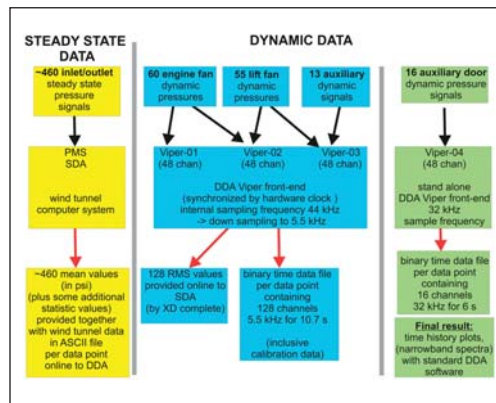


Figure 3: Schematic of the DNW data acquisition system

## The International Vortex Flow Experiment 2 in the DNW-TWG and the DNW-KKK

As contribution to the International Vortex Flow Experiment 2 (VFE-2) DLR has performed flow measurements on a  $65^\circ$  delta wing with sharp as well as with rounded leading edges. The wind tunnel tests comprised parallel measurements with Pressure Sensitive Paint (PSP) and Particle-Image Velocimetry (PIV) techniques in the TWG and also parallel measurements with Temperature Sensitive Paint (TSP), PIV techniques and an infrared camera and in the KKK.

The first vortex flow experiment was carried out in the years 1984 to 1986 on a cropped  $65^\circ$  delta wing with fuselage. The objectives were to provide high quality experimental data to validate numerical calculations of vortical flows. In the last two decades considerable progress has been achieved in the field of Computational Fluid Dynamics (CFD) and, therefore, a second international vortex flow

experiment was proposed. Since 2003 VFE-2 is being carried out by a special task group within the framework of the NATO Research and Technology Organization. Results of numerical state-of-the-art codes were compared with new experimental data obtained by modern measurement techniques. The work within VFE-2 also focuses on the flow investigation of delta wings with rounded leading edges.

The delta wing geometry chosen for VFE-2 is a NASA delta wing of  $65^\circ$  sweep angle (Figure 1). The thickness distribution of the configuration consists of a flat plate inner portion in combination with interchangeable leading edge segments. Within VFE-2 the sharp as well as the medium rounded leading edge was chosen. For the current tests in the TWG the delta wing model of 490 mm root chord length was provided by NASA Langley. Twice this size is the delta wing model of the Technical University of Munich used for the KKK tests.

PSP and PIV as well as TSP are able to capture a huge amount of experimental data during a wind tunnel test campaign. With PSP the pressure distribution on a whole surface can be determined giving much more insight in details of the flow topology than would be possible by discrete pressure taps. PIV provides instantaneous as well as averaged flow velocity fields in different planes of the flow and enables the detection of large and small spatial flow structures. With TSP the lines of laminar / turbulent transition in the boundary layer can be determined. The combined application of these methods can help to save wind tunnel costs in order to get the necessary data for flow analysis or comparison with CFD results.

In a first test campaign surface pressure distributions were measured in the TWG with PSP (Figure 2), which served as “pathfinder” tests. Their results gave a first information of the flow topology over the delta wing for a large range of angles of attack. In the same wind tunnel PIV measurements were performed in a second test campaign for which specific angles of attack and locations of the measurement planes above the delta wing were selected on the basis of a first analysis of the PSP results. The measured velocity fields provide detailed information of the instantaneous and time averaged flow fields. The applied stereo PIV setup (Figure 3) allows for flow velocity measurements above the delta wing within planes perpendicular to the model axis at different chord stations. The light-sheet and the cameras can be translated along the model axis during wind tunnel operation. The arrangement also incorporates rotary plates in order to adjust quickly the setup for different angles of attack. The model was coated with a specific paint to reduce laser light flare on the model surface which allow for PIV measurements down to the surface.

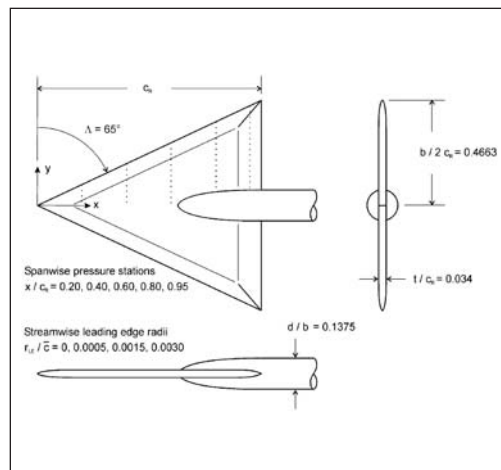


Figure 1: Definition of the geometry of the delta wing

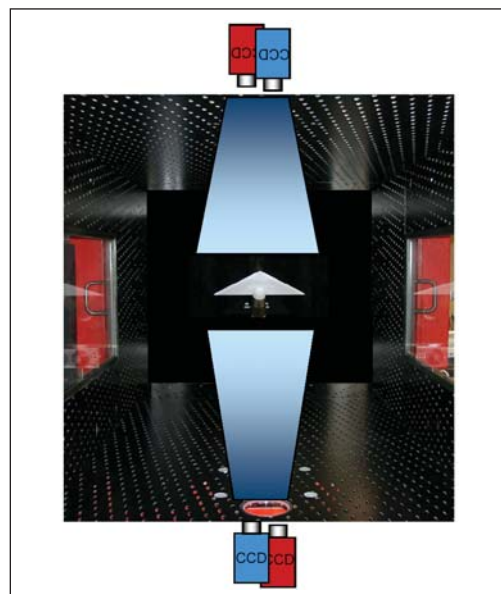


Figure 2: PSP arrangement and the coated delta-wing model in the test section of TWG



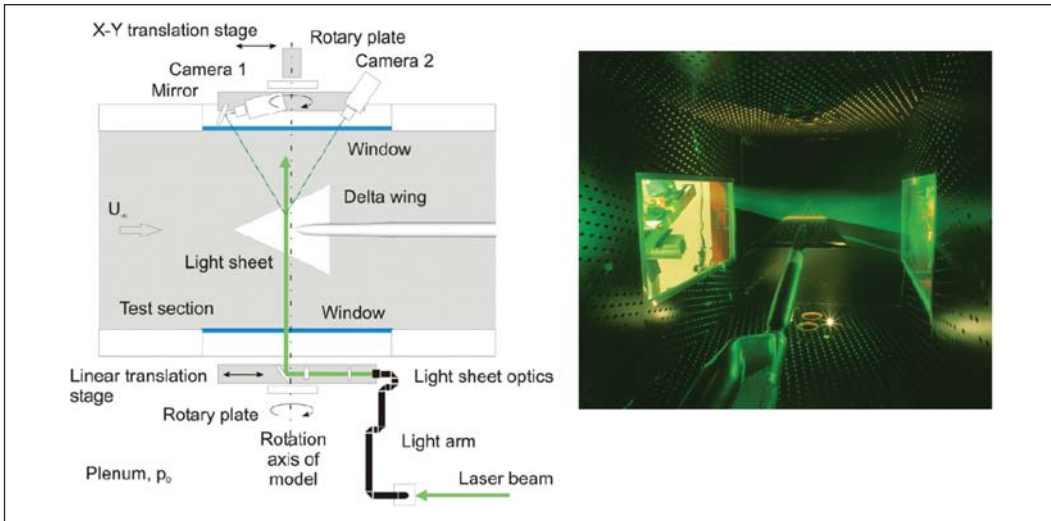


Figure 3: Stereoscopic PIV arrangement at the TWG and picture from inside the perforated test section showing the coated delta wing, light sheet and the two lateral schlieren windows

For the VFE-2 delta wing configuration a specific flow topology occurs in the rounded leading edge case. In addition to the well known outer primary vortex another inner primary vortex develops. Figure 4 shows the PIV and PSP results for  $Ma = 0.4$  and  $Re_{MAC} = 3$  million (with respect to mean aerodynamic chord) and angle of attack of  $13^\circ$ . In this case the flow separates at the leading edge first at  $x/c_r = 0.5$  and the primary vortex is formed, which produces a strong suction peak in the pressure distributions. However, another weaker suction peak can be detected more inboard with a highest peak height just downstream the origin of the outer primary vortex. The velocity distributions at  $x/c_r = 0.6$  reveal that this suction peak is produced by another inner vortex co-rotating to the outer one. This vortex develops from a thin vortex structure which occurs more upstream close to the surface, at  $x/c_r = 0.4$ . Instantaneous PIV results show that this vortex structure consists of several small co-rotating vortices spreading in the spanwise direction. Between the outer primary vortex and the inner vortical structure the flow re-attaches to the surface and separates again so that vortices of the inner vortical structure detaches from the surface, at  $x/c_r = 0.5$ . These vortices merge and a circular inner vortex is formed such that two co-rotating vortices of approximately the same size can be observed at  $x/c_r = 0.6$ . Further downstream vorticity is fed only into the outer primary vortex and the strength of the inner vortex gradually decreases, whereas the inner and the outer vortex remain separated and do not merge.

The tests in the KKK were originally planned to obtain velocity data at high Reynolds numbers. However, as it came out that the knowledge of laminar / turbulent transition in the boundary was essential to compute the flow around the delta wing more precisely the objectives of the KKK campaign were modified. Although, the intended delta wing model for the KKK tests was not especially

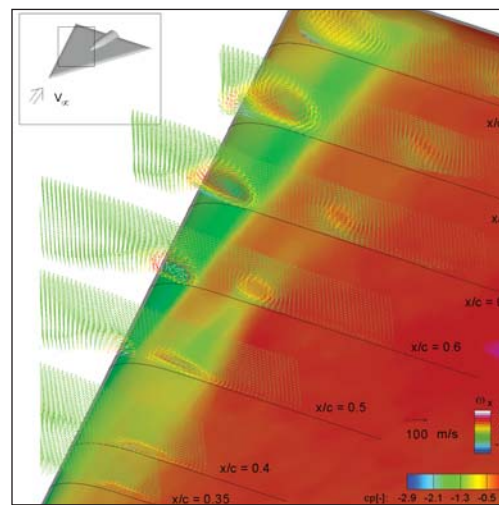


Figure 4: Time averaged pressure, velocity and vorticity distributions above the delta wing with rounded leading edges. The in-plane velocity vectors are plotted in different planes perpendicular to the delta wing axis. The color of the vectors corresponds to the out-of-plane vorticity. The colors at the surface are related to the local pressure coefficient

designed for transition measurements, it was decided to apply also the TSP and infrared techniques. For all tests in the KKK the model was coated with the temperature sensitive paint.

While the infrared technique works very well at temperatures higher than 200 K (low Reynolds numbers) the TSP technique can be applied at temperatures lower than 200 K (high Reynolds numbers). In both cases, these non-intrusive observation techniques detect boundary layer transitions on a model by measuring the temperature differences generated between laminar and turbulent boundary layers due to the difference of their convective heat transfer coefficients. However, in the case of TSP, the naturally generated temperature difference is usually too small to create a large enough temperature difference on a model made of aluminium for the cryoTSP technique. Therefore, one needs to apply artificial enhancement of the laminar-to-turbulent temperature difference for cryogenic testing. In this measurement, the delta wing model was stored in the model-conditioning room beneath the test section and warmed up.

Figure 5: TPS result for the delta wing with rounded leading edges showing laminar / turbulent transition of the boundary layer.

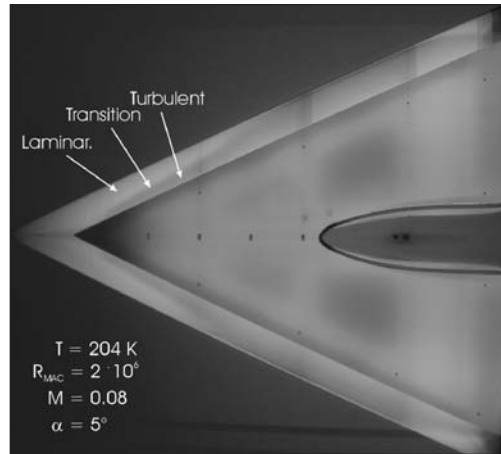


Figure 6: Infrared image of the delta wing with rounded leading edges showing laminar / turbulent transition of the boundary layer.

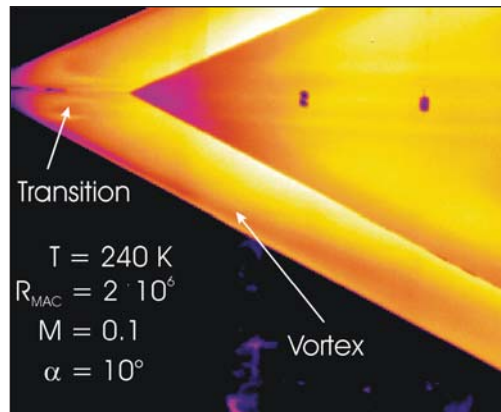


Figure 7: Stereoscopic PIV arrangement at the KKK. Camera 1 is located inside the wind tunnel 4 m downstream the model within a temperature controlled camera housing.

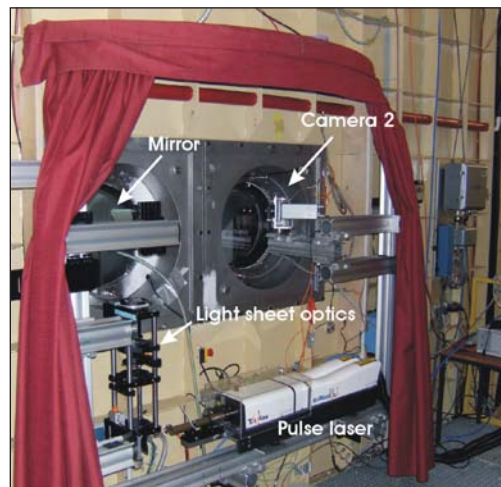
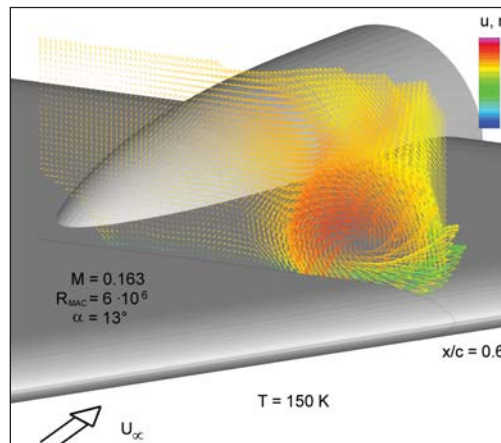


Figure 8: Time averaged in-plane velocities (vectors) and out-of-plane velocities (vector color) at  $x/c_f = 0.6$  above the delta wing with rounded leading edges obtained in the KKK at  $T = 150$  K and  $\alpha = 13^\circ$ .



Then the model was quickly lifted up to the test section which was kept at the test temperature (205 K and 240 K) and the tunnel started blowing immediately. After the tunnel reached the test condition, the run images were obtained using the temperature difference between the model and the flow before the model temperature could adapt to the flow temperature.

Figures 5 and 6 show results from TSP and infrared techniques respectively. In both results the inhomogeneous cooling of the model caused by its varying thickness and hollow spaces inside the model can be seen. However as indicated in Figure 5 the laminar / turbulent transition can be clearly identified at the leading edge for a small angle of attack of  $5^\circ$  when no vortex is formed. At  $\alpha = 10^\circ$  the primary vortex occurs and produces also a temperature signal at the surface (Figure 6). This complicates an interpretation of the results and makes a further analysis of the images necessary.

To investigate the flow topology above the delta wing model with rounded leading edges at higher Reynolds numbers PIV was applied in the KKK under cryogenic conditions. The realized stereo PIV setup is shown in Figure 7. A single measurement plane was used at  $x/c_f = 0.6$  perpendicular to the model axis for an angle of attack of  $13^\circ$ . Figure 8 shows a result taken at a flow temperature of 150 K and  $Ma = 0.165$ . The primary outer vortex as well as a weak inner vortex can be observed.

The presented results show that the measurement techniques such as PIV, PSP and TSP can be powerful tools for flow investigations in industrial wind tunnels as the TWG or KKK. However, the activities within VFE-2 show also useful interactions between computational and experimental disciplines. Using the PSP results it was also possible to perform a flow computation which also show an inner vortex. In turn the CFD result could be used for setting up the PIV system at the TWG. The first computations show also that the knowledge of the locations of laminar / turbulent transition is required to be able to computationally predict the flow more precisely which led to the TSP and IR measurements in the KKK.

Contributed by R. Konrath, Ch. Klein, U. Henne, W. Sachs, A. Wiedemann, D. Otter, A. Schröder, J. Agocs, M. Mattner, Y. Egami, U. Fey, K. de Groot (all DLR)



## Highlights of Project Work

### Environmental Engineering

#### The European Project MEXICO

In the context of the EU project MEXICO (Measurements and Experiments in Controlled Conditions), tests on a wind turbine model with three blades and a diameter of 4.5 meters were performed in the DNW-LLF open 9.5 m x 9.5 m test section. The project team consisted of a consortium of nine research partners in five countries, including the Netherlands, Denmark, Sweden, Greece and Israel. The Energy research Centre of the Netherlands (ECN) was the project coordinator.

The dimensions and complexity of wind turbines have increased significantly over the past few years. The aerodynamic models in existing computer programs contain too many unknown elements. In order to reduce the design risks and costs, detailed measurements on the rotor blades are needed. Over the past few years, field measurements have been performed in regions around the world, but unfortunately it is difficult to distil usable data from these measure-

ments. This is due to fluctuating wind speeds and directions in the free atmosphere, which leads to a large uncertainty when interpreting the data. In a wind tunnel it is possible to control constant wind speeds and directions. A disadvantage of most wind tunnels is that small models of wind turbines must be used by which the results are not representative for full scale dimensions. For this reason the LLF with its largest test section dimension has been chosen for testing.

The turbine model was mounted on a tower in such a way that the rotor axis was located at tunnel centre line (Figure 1). The tower was mounted on the external balance for setting of the wind direction (yaw) and measurement of all forces and moments on the turbine/tower. The wind speed in the open 9.5 m x 9.5 m test section varied between 5.5 and 30 m/s, and the wind direction was set at yaw angles between plus 30 and minus 30 degrees. The rotor speed was controlled electrically and was usually kept constant at 424.5 rpm (7 Hz).

Figure 1: Wind turbine model mounted on the external balance in the open-jet test section. The wind tunnel flow is from right to left

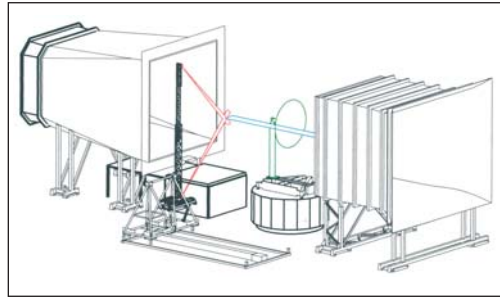
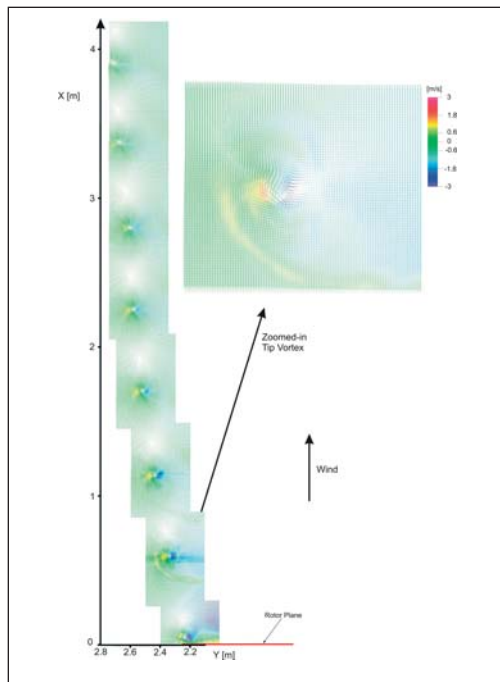


Figure 2: MEXICO PIV set-up. The wind tunnel flow is from right to left



Figure 3: Top view of the wake structure of a wind turbine as a composite of 15 PIV results



The test data mainly consisted of measurements of blade pressures as well as the details of the air flow around the blades and rotor. Therefore the blades were instrumented with 148 high response pressure sensors to measure the fluctuating pressure distributions around the blade airfoils. The pressure sensors were connected to PCBs (Printed Circuit Boards) in the blades, from which the data was led (digitally) over a slip ring into the data acquisition system located in the non-rotating part of the model. All three blades were also instrumented also with strain gauges at the blade root to measure the root bending moments.

The flow field in the vicinity of the turbine blades was measured by means of Particle Image Velocimetry (PIV). In particular the flow upstream of the rotor plane, within the rotor plane as well as in the wake

was the objective of the investigation. The influence of wind speed and crosswind situations on the performance of the turbine rotor was also part of the measurements.

Before the testing program started, the consortium partners determined several representative positions within the entire flow field from where the data should be obtained. All measurement locations were within a horizontal plane in the height of the rotor axis. The three components of the flow field in this plane were determined by means of PIV. The flow field thus determined was investigated at three different wind speeds and under two crosswind conditions. In addition, the partners were interested in the behavior of the flow depending on the rotor blade position.

In order to determine three velocity components, the measurements were carried out with a stereoscopic set-up of the cameras. One camera was directed from above to the horizontal light sheet, the second camera recorded its images from underneath. This configuration was fixed and was, in its entirety, moved by means of two traversing systems from one measuring location to the others, see Figure 2. This fixed set-up of cameras and light sheet allows the system to be calibrated in advance and outside the wind tunnel, thus avoiding time consuming re-calibration.

The line-of-sight angle of both cameras to the normal of the measurement plane is 45 degrees. This PIV set-up contributes an equal resolution of all three velocity components, i.e. the two in-plane components and the out-of-plane component.

The result of a PIV measurement is a vector map of the flow field area on which the cameras are focused. A composite of a number of vector maps is shown in Figure 3. This figure represents a cross section of the rotor wake, in which the helical structures of the tip vortex lines of all three blades are embedded. The vector lengths and the vector directions indicate the in-plane wind components; the color of the vectors indicates the out-of-plane component. The figure clearly shows the typical behavior of wind turbine tip vortex structures, i.e. an increasing diameter of the vortex line spiral. This behavior is due to the withdrawal of momentum from the atmospheric wind field by the wind turbine. The resulting decreased wind speed downstream of the rotor plane is the transportation velocity of the vortices and can be derived from the corresponding rotor rpm and the distance between two adjacent tip vortices. The test conditions represented in Figure 3 lead to a wind speed reduction of about 23% just behind the rotor plane.

ECN states that the analysis of the results of the tests is still incomplete, but has already produced very unique findings. They expect that they will continue to use the data from this test for years to come



## Technical Status

### Engine Simulator Monitoring at the LLF

Turbofan Propulsion Simulators (TPS) and air motors are used in wind tunnel tests to simulate the flow conditions of the real engines of an aircraft. Scaling the real engine to model scale leads to engine simulators with a small volume and high power given the limited size of the wind tunnel models. This results in an engine design with a number of critical parts, e.g. the high-speed bearings of a TPS (RPMs up to 60,000). The simulation of the real engine requires the air motor to be run at the same RPM as the real engine. This means that the scaled bearing has to have a higher performance and endurance than the real engine's bearing. As a consequence, the bearing temperatures have to be closely watched since they provide information on a possible failure of the bearing. To safeguard the TPS/air motor and model several so-called critical parameters are monitored. Apart

from the bearing temperature these parameters include the RPM, the acceleration levels, the inlet pressure, etc. The Engine Simulator Monitoring (ESM) system will observe all critical parameters of the TPS/air motor units and will generate a warning to the operator if critical situations arise. The ESM will stop the TPS/air motor if a pre-set limit is reached.

The first engine monitoring systems were designed and manufactured by NLR about twenty years ago. This first generation of engine monitoring systems consisted of mechanical parts and hard-wired electronics only. This system could only generate an emergency stop and log the critical parameters with a plotter on paper. Later on a new engine monitoring system was designed and manufactured for the LLF. For this system partly a software solution was chosen. This second generation system also has a PC based operator interface. In addition to the first generation system this system could generate

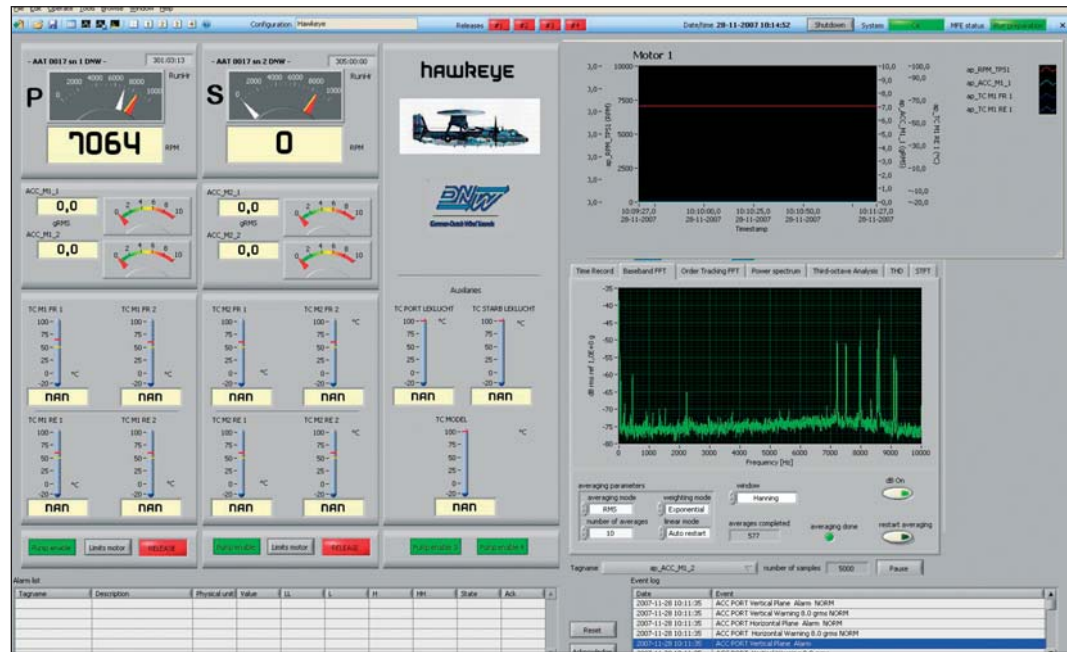


Figure 1: Engine simulator monitoring system at the LLF

warnings and log the critical parameters electronically, so data analysis became possible. The second generation of engine monitoring system was increasingly more difficult to maintain due to obsolescence of certain electronic components and the lack of spare parts. This is why DNW ordered a new, third generation engine monitoring system, which was designed and manufactured by NLR.

Two systems were put into operation and have successfully been used in the LLF and the engine calibration facility ECF. The new ESM system is capable of safeguarding up to four TPS/air motor units simultaneously. The system monitors and logs RPM, acceleration, bearing temperatures and several other parameters of the engine. The system is used as a stand-alone system; however data acquired by the system is made available for use by other wind tunnel subsystems like the overall data acquisition system. The capabilities of the system are further enhanced by digital and analog input and output channels and online data analysis tools such as a Fourier analysis and adjustable tracking filters. This makes it possible to trend-watching for the parameters. Two systems were put into operation and have successfully been used in the LLF and the ECF.

### Development of the Viper System Since the Year 2000

A description of the DNW dynamic data acquisition (DDA) system which revolutionized the quality and efficiency of the available data acquisition capacity in particular at the LLF of DNW was described in the Annual Report of the year 2000. At that time the new DDA system with a name "Viper" was

introduced with the primary aim of dealing with the large amounts of data generated by the use of the phased microphone array technology for acoustic measurements. Since then a number of new applications have been introduced, alongside with upgrades of the Viper system triggered by the novel applications as well as by the increased use of the system in the other tunnels of DNW. This article describes a number of significant changes that have taken place, as well as some of the projects that have benefited from the DDA enhancements.

The most obvious change is the number of available channels of the DDA systems. When the system was first introduced, the availability of 128 channels was a stated goal and an achievement. At present, the total number of available channels is 240, based on five front-ends of 48 channels each. The separation into five single front-end units enables the parallel use of the DDA system in different applications and different locations at the same time. Furthermore, since the Viper system has become a virtual standard for dynamic data acquisition systems for acoustic applications, more compatible units are available at both parent institutes DLR (seven front-ends) and NLR (three front-ends) as well as institutes of higher learning elsewhere in the world. Together with the systems from DLR and NLR there is potentially the maximum number of 720 channels available.

At the same time as the external aspects of the system were expanded, the system's internal capabilities have also been increased by continuous improvements. The sample rate for data acquisition has been increased from 200 kHz to 250 kHz. This has been possible due to improvements in the CPU units and the increase of the storage space and net-

working capability in the internal PC hardware. Even when all the channels are acquiring data at the maximum rate of 250 kHz, the orders of magnitude increase in hard disk capacity and transfer speed and networking speed (from 100 Mb/s to 2 x 1 Gb/s) assure continuous uninterrupted operation.

Furthermore, the data acquisition capacity has been backed up by commensurate storage upgrades. Instead of storing up to 40 GB information on digital tapes as was the case in the initial version of the system, data is now stored on a 4 TB dedicated file server (extendable to 10 TB), accessible through a 1 Gb/s network online. All this data is processed by a computer cluster upgraded from simple PCs to state-of-the-art work stations and enabling near online visualization of acoustic measurement results within minutes of the actual measurement.

The advantages of the increased hardware capacity can only be fully appreciated when the software makes adequate use of this. For that the internal operational software monitoring the DDA operation and signal values has been expanded to, among other enhanced features, provide for real time digital filtering, real time true RMS calculation etc. This improvement has been of significant advantage when continuous monitoring and online processing of the rotating shaft balances (RSBs) is needed in critical tests with models of propeller aircraft (A400M, Hawkeye). The advantages of the near to online processing capabilities are particularly helpful when the test productivity aspect in the DNW tunnels LLF, LST, NWB and HST is taken into consideration, since the Vipers can be fully integrated with the operating systems of these tunnels.

Although the Viper systems have found their use in monitoring and measuring dynamic signals in a wide variety of dynamic and rotating systems like RSBs and dynamic airfoil loading by wakes and gusts, the main field of application is still that of microphone array measurement. DNW currently possesses a number of arrays that can be utilized with the help of the Viper system. There are two new sets of 4 m x 4 m out-of-flow microphone array frames (96 to 140 microphones each) and two new 1 m x 1 m flat wall arrays with 144 microphones each. These wall arrays can be utilized simultaneously in the wind tunnel for purposes such as directivity detection or simultaneous measurement of different locations (e.g. from the ceiling and from the side wall of a closed test section). This can be accomplished with only three front-end units through the application of adequate channel A-B switching units, leaving other units available for alternative use.

The improvements in the hardware and software of the Viper system that have been implemented over

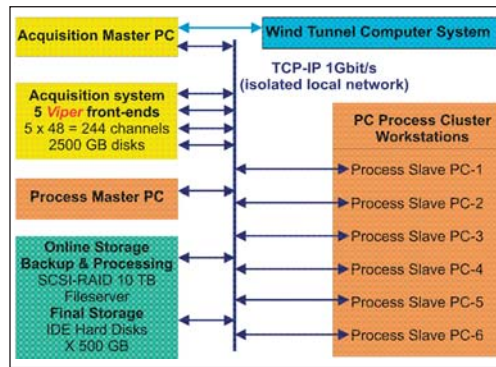


Figure 2: Schematic of the Viper system

the years have helped DNW to maintain its leading position in simulating dynamic aerodynamic phenomena in wind tunnels, without paying the penalty of increased operational complexity. The developments were undertaken in such a way as to enable an increase in the data quantity and quality without straining the test team with extra responsibilities during the test. However, because the flexibility of the system enables DNW to satisfy a wide range of requirements, the team's responsibilities do increase during the planning stage as the test planners have to make additional choices regarding those requirements.

### Aircraft Maneuvers Realistically Simulated in a Wind Tunnel

During the expensive process of aircraft development it is highly desirable to obtain information about the future handling qualities of the aircraft already at a very early stage. For the experimental determination of the corresponding dynamic derivatives a new combined motion test capability was developed at DNW, with support from its parent institute DLR, for its wind tunnel NWB in Braunschweig, using a six degree-of-freedom test rig called "Model Positioning Mechanism" (MPM) as an improved successor to the older systems Mobile Oscillatory Derivative Balance (MOD) and Oscillating Motion Support (OMS).

This test rig can be used for oscillating the wind tunnel model about one body axis through a sinusoidal motion as well as for combined motions to simulate realistic flight maneuvers, e.g. a dutch-roll (Figure 3). Besides its application for dynamic tests the MPM is also well-suited for static tests in combination with ground effect simulation.

The major characteristic of the test rig is its high dynamic capability combined with high and nearly constant stiffness over the whole workspace which spans 1100 mm in flow direction, 300 mm in lateral direction and 500 mm in heave direction. To meet the demands of large amplitude and high-rate



Figure 3: Aircraft model suspended from the MPM at the NWB

arbitrary motion a six degree-of-freedom parallel kinematic mechanism was developed with the following advantages compared to a conventional serial axes arrangement:

- Higher dynamics despite identical input power because lower weights are being moved
- Higher accuracy because errors in parallel kinematics exert less effect
- Lower cost due to simpler construction and identical components for each axis
- Lower demands on tolerances for production and assembly because geometric transformation takes the place of axial alignment

The kinematic mechanism consists of a movable platform (Stewart Platform) which is linked to the wind tunnel fixed base by six constant length legs - joined with the platform as well as with six carriages which can move along parallel guiding rails, so that the position and orientation of the platform can be adjusted. The six carriages run independently of each other on each guiding rail, allowing a displacement within six degrees of freedom. Because each guiding rail is shared by three carriages, the design is simplified and has fewer components than previous versions.

For control of the MPM NC milling machine hardware, Sinumerik 840D, in combination with adapted software is used. To avoid a conventional ballscrew drive with its elasticity in the drive chain the axes are brought into motion by application of the linear direct drive technology. Altogether six Simodrive 1FN3 linear motors are used, allowing acceleration up to 2.5 g. The accuracy of the system in pivoting angles is  $<0.005^\circ$ . The first eigenfrequency at the top of the sting is above 20 Hz. The test rig allows a payload of up to 5000 N.

## Vibration Control System of the DNW-TWG Motor and Compressor

The TWG power train (Figure 4), consisting of a motor, a drive shaft, and a compressor, mounted on a heavy seismic mass system needs permanent vibration control in order to avoid fatigue and damage and to monitor health condition. The old system, which evolved over time, had become unreliable and no longer complied with current technical requirements. Technically unfounded emergency stops occurred with increasing regularity, which increased wear and tear and resulted in unnecessary tunnel downtime. In addition, it was often difficult to perform fault tracking, which was time-consuming because no plausible reason could be found.

High-frequency compressor casing resonances raised the measured total value of oscillation amplitude above the threshold for emergency stops. These high-frequency contributions depend on temperature and pressure, which make it difficult to reproduce and predict them. The new control system uses the total value to calculate the effective oscillation speed that corresponds to the momentary rotation rate (first order). This result is much more representative for a possible imbalance and running conditions of the compressor, which is why this is recommended by the manufacturer.

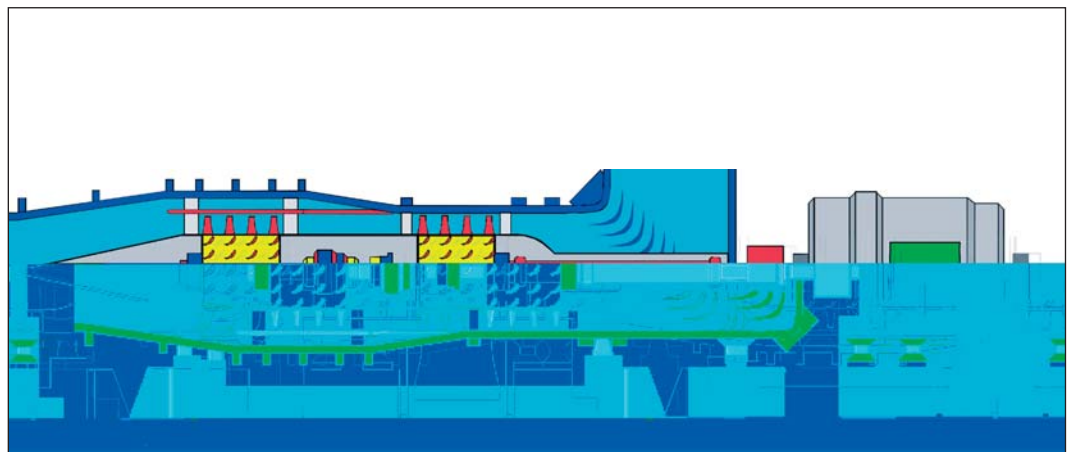


Figure 4: Schematic illustration of power train



The number of sensors mounted on the compressor was doubled. Two sets of four sensors now monitor vibrations in the horizontal and vertical directions, close to the compressor bearings. Observation of both directions is necessary because of the different horizontal and vertical damping properties of the compressor foundation.

Before the upgrade, only the drive shaft side of the motor was observed. Since the upgrade, vibration control sensors monitor the horizontal and vertical vibration components directly at both bearings (Figure 5) and at two points of the shock-absorber mounted concrete block. The measured frequency spectrum shows that resonance contributions are negligible. This is the reason why the total oscillation speed at all frequencies is used as a health monitoring and decision criterion.

In addition to the permanently installed sensors, a mobile vibration control system has been purchased. This system is used regularly for inspecting other rotating components of the TWG. While the improved monitoring capacity does not avoid damage, it improves the early recognition of damage, should it occur.

### Increased Operational Efficiency of the DNW-KKK

Operating a cryogenic wind tunnel like the KKK requires well-prepared operating procedures with respect to safety and economy. The large amounts of liquid and gaseous nitrogen ( $LN_2/GN_2$ ) must be handled by three operators who need to assist one another in the event of reduced oxygen concentration. Liquid nitrogen pumps, valves and evaporators have to be controlled carefully. Imperfections in the thermal tunnel insulation require permanent nitrogen injections to compensate for the effects of rising temperatures. As a consequence, any idle time of the cooled down tunnel must be avoided,



Figure 5: Vibration sensor (silver with dark cable) and temperature sensor (in front, grey cable) on the TWG compressor

especially overnight and during weekends. Moreover, the purging procedures aimed at removing humidity by means of nitrogen or dry pressurized air need to be optimized.

The above-mentioned issues have been addressed with a number of measures that support a safe and cost-effective two-shift/three-person operation by automating the control and handling of processes.

The following figure 6 shows the revised structure of the KKK systems for data acquisition and reduction and for tunnel operation and control. Both systems are fully integrated. This increases the overall reliability and safety of the tunnel. The following sections describe two new features that increase the operational efficiency of the KKK:

- The measured forces can actuate the Mach number control in order to avoid balance overload during automatic operation;
- The model lock lift system is kept in constraint by the model position in order to prevent accidents due to operational errors.

To improve the reliability and performance of the tunnel control system, the Siemens WinCC was updated from version 5.0 SP2 to version 6.0 SP4. The new version runs on Windows XP or Server

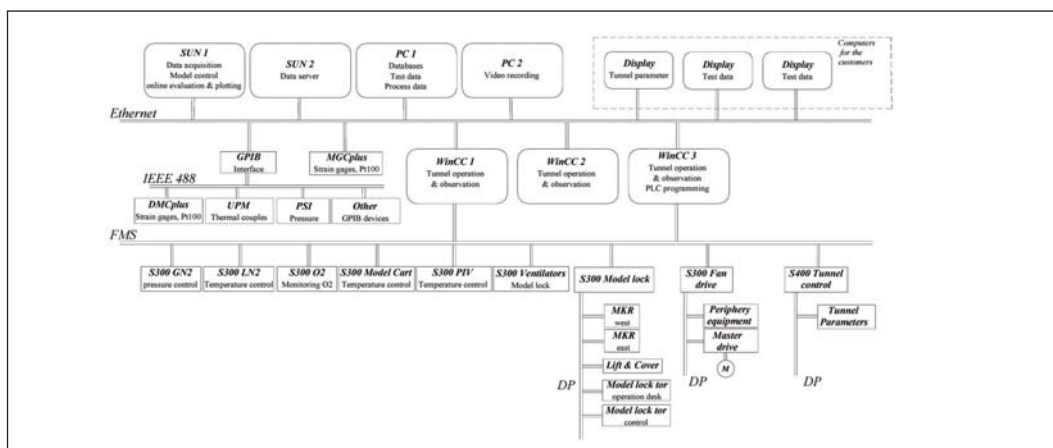


Figure 6: Structure of the KKK data acquisition and control system

2003. The data storage format was changed from Sybase SQL 7 to the powerful real-time database Microsoft SQL Server 2005. The function can be expanded with Visual Basic for Applications, as well as C-programs. The PLC programming environment was also upgraded from version 5.0 to version 5.4 SP1. The computers were replaced with state-of-the-art computers equipped with dual-core processors and high-capacity disks.

Some customers want to have more information about the test process than just the aerodynamic coefficients that were evaluated online. To meet this need without extra workload for the operators, the proven client-server model was expanded. In this set-up, the server obtains all the process data via WinCC. In addition, three extra computers were provided to enable customers to observe the tunnel process.

A main factor that affects the productivity during the cryogenic operation is the configuration change, because the model needs to be warmed up in the model lock for every configuration change. Moreover, the model needs to be cooled down again after the model modification. An automatic conditioning process was realized to reduce the lost time for model conditioning. As a result, the model can be conditioned (cooled down or warmed up) automatically in the model lock during night or weekend. The morning shift can change or test the

model directly without waiting. Although technically possible, conditioning the tunnel is not practised for safety reasons. The standard test procedures include Re-number (i.e. temperature) variations. This means that starting at higher temperatures after idle periods can be accepted. The model conditioning process efficiency has been additionally improved by the installation of an advanced supply system for dry pressurized air.

### Extension of the DNW-RWG Simulation Range with the New Mach 2 Nozzle

The RWG at Göttingen is a Ludwig Tube with two storage tubes and a set of fixed nozzles. This set-up enables the tunnel to realize Mach numbers up to 6.8. Tube B can be heated to avoid condensation at Mach 5 and above. Although the testing time for this intermittent wind tunnel is short (see the table below), the excellent accessibility and low operating costs – compared to a continuous facility – make the RWG an ideal tool for fundamental research tests with frequent model and test set-up changes.

The lowest Mach number used to be 3, which left a gap between this tunnel and the other supersonic DNW tunnels TWG and SST. As a result of increased requests for Mach 2 with respect to

Key Technical Parameters		Tube A		Tube B
Maximum storage pressure $p_{\text{tube 0}}$	[MPa]	1.5		4.0
Maximum storage temperature $T_{\text{tube 0}}$	[K]	Ambient		670
Mach numbers Ma		2.0	3.0, 4.0	5.0, 6.0, 6.8
Unit Reynolds number $Re_1$	$[10^6/m]$	18 – 125	8 – 80	2 – 50
Test section cross-section area	[m]	0.34 x 0.35	0.5 x 0.5	Ø 0.5
Testing time	[s]	0.4		0.3

Key technical parameters of the RWG

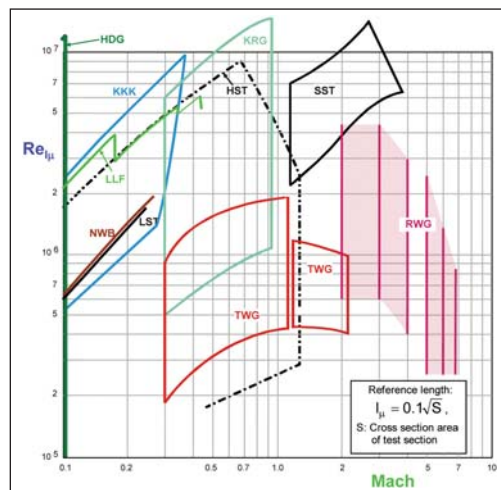


Figure 7: Extended simulation range of the RWG compared to the other wind tunnels of DNW

supersonic aircraft and missiles, DNW and DLR jointly built another nozzle. The key parameters are listed in the table. The sidewalls are equipped with flanges to support sensors and large schlieren and infrared (Germanium) windows. The model support is common for all nozzles.

Due to the existing tube diameter that limits the mass flow, the cross section had to be reduced. Nevertheless, as the pressure can be raised to 15 bar, the standard Reynolds number covers quite an interesting range and meets the requirements of the main customer DLR. As the diagram in Figure 7 shows, DNW thus has improved its testing capabilities from subsonic to hypersonic within the internal pool of facilities.

The new test section was put into operation at the end of 2006. In the meantime, research projects were started on innovative missile drag reduction and supersonic wing boundary layer control, including Mach 2.

The experimental investigation of the delay of laminar-turbulent transition on a supersonic swept wing by suction was carried out within the framework of the EC project SUPERTRAC. The investigation was conducted by the DLR Institute of Aerodynamics and Flow Technology in the new Mach 2 nozzle of the Ludwig tube facility. The tests were completed successfully. Figure 8 shows the SUPERTRAC model in the test section of the RWG. The black part on the surface is the insert used for heat flux measurements.



*Figure 8: SUPERTRAC model in the test section of the RWG*

# Acknowledgement

All staff members who contributed to this issue of DNW's Annual Report are gratefully acknowledged. In particular, special mention is given to Piaggio, the DLR Institute for Aerodynamics and Flow Technology and ECN for their contributions.

# Status of the Foundation

## General

The Foundation DNW (German-Dutch Wind Tunnels) was jointly established in 1976 by the Dutch National Aerospace Laboratory (NLR) and the German Aerospace Center (DLR), as a non-profit organization under Dutch law. The main objective of the organization is to provide a wide spectrum of wind tunnel tests and simulation techniques to customers from industry, government and research. DNW owns the largest low-speed wind tunnel in Europe, the LLF, and also operates the major aeronautical wind tunnels of DLR and NLR, which are fully integrated into the DNW organization. The wind tunnels operated by DNW are grouped into two Business Units "Noordoostpolder/Amsterdam" (NOP/ASD) and "Göttingen und Köln" (GUK).

## The Board of DNW

The Board of the Foundation is composed of members appointed by NLR, DLR, and the German and Dutch governments. At the end of 2006, the Board consisted of:

Ir. F. Abbink, NLR, Chairman  
Prof. Dr.-Ing. J. Szodruch, DLR, Vice-Chairman  
Reg.Dir. A. Drechsler, German Federal Ministry of Education and Research, BMBF  
Prof. B.A.C. Droste, Netherlands Agency for Aerospace Programmes, NIVR  
Drs. L.W. Esselman, R.A., NLR  
Dir. BWB K. Heyer, German Federal Ministry of Defense, BMVg  
Dipl.-Ing. H. Hüners, DLR  
Ir. P.J. Keuning, Dutch Ministry of Defense  
Secretary: Ms. S. Pokörn, DNW

## Advisory Committee

The Advisory Committee, representing the aerospace industry and research establishments, advises the Board of DNW about the industry's long-term needs. At the end of 2006, the Advisory Committee consisted of:

Prof. Dr.-Ing. S. Levedag, DLR, Chairman  
Dipl.-Ing. A. Flaig, Airbus Deutschland GmbH  
Prof. Dr.-Ing. J. Klenner, Airbus  
Dr. B. Oskam, NLR  
M. Polychroniadis, Eurocopter France  
Prof. Dr.-Ing. C.C. Rossow, DLR  
L. Ruiz-Calavera, EADS CASA

## The Board of Directors

DNW is managed by a Board of Directors consisting of:

Director: Dr.-Ing. G. Eitelberg, DLR  
Deputy Director: Ir. C.J.J. Joosen, NLR

## Organizational structure

At the end of 2006, the permanent staff of DNW totalled 124 employees, 60 of them (including the Director) were seconded by DLR, 64 of them (including the Deputy Director) were seconded by NLR. Business Unit NOP/ASD had 92 employees and GUK 32. About two-thirds of the staff (82) were posted in the Netherlands and one-third (42) in Germany.

K.-W. Bock, M. Bruse, M. Jacobs

*Aerodynamische Messungen für Forschung und Entwicklung in DNW-Windkanälen*  
Measurement 2006, Göttingen, 15 to 17 February 2006

J. Takens, I. Philipsen

*Improvements in Balance Calibration at DNW*  
Fifth International Symposium on Strain-Gauge Balances, Aussois, France, 09 to 12 May 2006

M. Laban, J. Maseland, H. van der Ven (all NLR) and J.W. Kooi

*Development of CFD-Based Interference Models for the DNW HST Transonic Wind Tunnel*  
25<sup>th</sup> AIAA Aerodynamic Measurement Technology and Ground Testing Conference, Hyatt Regency, San Francisco, USA, 05 to 08 June 2006

M. Rein, G. Höhler, A. Schütte (all DLR), A. Bergmann, T. Löser

*Ground-Based Simulation of Complex Maneuvers of a Delta-Wing Aircraft*  
25<sup>th</sup> AIAA Aerodynamic Measurement Technology and Ground Testing Conference, Hyatt Regency, San Francisco, USA, 05 to 08 June 2006

C.J.J. Joosen

*Pressure Measurement Systems at DNW-LLF*  
42<sup>nd</sup> SATA Conference, Istanbul and Ankara, Turkey, 04 to 08 June 2006

G. Eitelberg

*The Importance of Wind Tunnel Testing on Aircraft Design.*

Joint EWA and DESider Workshop on Validation of Numerical Methods in Aerodynamics, Stockholm, Sweden, 13 and 14 June 2006

D. Eckert, G.H. Hegen, W. Kühn (Airbus)

*Wall and Support Interference Effects on Low Speed Measurements with a Propeller Powered Transport Aircraft*

ICAS Congress 2006, Hamburg, 03 to 08 September 2006

K.W. Bock

*Repair and Refurbishment of the Transonic Wind Tunnel Drive Motor*

106<sup>th</sup> STAI, TsAGI, Moscow, Russia, 17 to 19 September 2006

T. Löser, A. Bergmann

*Capabilities of Deployment Tests at the DNW-NWB*

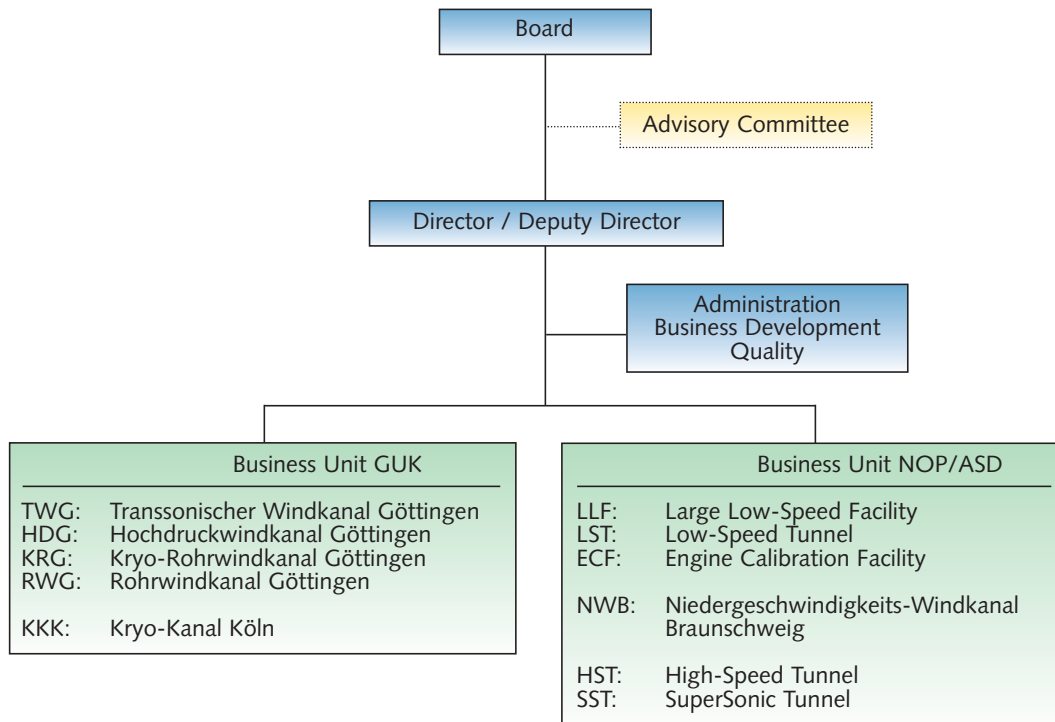
NATO AVT-133 (RSM-018), Vilnius, Lithuania, 02 and 03 October 2006

K. Pengel

*Rotorcraft Testing in DNW*

2006 International Rotorcraft Workshop, Konkuk University, Seoul, Korea, 17 to 19 December 2006

# Organization of DNW



## Royal visit at the LLF on 01 November 2006

After discussions in the Hague and a visit to Amsterdam, on the third day of their state visit His Majesty King Abdullah II and Queen Rania Al Abdullah of the Hashemite Kingdom of Jordan paid a visit to the LLF, accompanied by their royal host Queen Beatrix of the Netherlands.

Owing to their busy schedule the visitors travelled by helicopter that landed on the premises of the NLR where Queen Beatrix' bus was waiting to take the delegation to the LLF. Fred Abbink and Georg Eitelberg, chairman and director of DNW, guided the guests through the facility where a running JSF test was briefly interrupted to demonstrate the work of DNW. Georg Eitelberg found an attentive listener in King Abdullah, who, a pilot himself, proved to be very interested in the testing procedures applied at the LLF.

The brief visit ended with the signing of the guest book by Queen Beatrix and King Abdullah.





# Celebration of a long lasting partnership

Airbus and DNW have been working together for 25 years in their drive toward commercial and technological success since the first paid Airbus test in 1981.

On 15 November 2006 the partnership of both companies was celebrated before an audience of industry, government representatives and personnel of Airbus and DNW.

After a greeting by Hans de Groene of the Dutch Ministry of Economic Affairs, Alain Garcia (Exec VP Engineering of Airbus), Fred Abbink (Director of NLR) and Joachim Szodruch (Member of the Board of DLR) presented their views on the future of aviation.

Innovation in wind tunnel simulation was the theme of a dialog between Axel Flaig (VP Aerodynamics of Airbus) and Georg Eitelberg, pinpointing the requirements for future aircraft development.

The tour of the facility and parking hall, featuring several Airbus models and model engines, was followed by further discussions among the participants over a dinner with live music.



# Wind Tunnels Operated by DNW

## General Inquiry

Joost W. Kooi  
Business Development

E-mail: [joost.kooi@dnw.aero](mailto:joost.kooi@dnw.aero)  
Phone: +31 527 24 8505  
Fax: +31 527 24 8582



HST, SST  
Anthony Fokkerweg 2  
1059 CM Amsterdam  
The Netherlands

Contact: G.H. Hegen  
Phone: +31 527 24 8519  
Fax: +31 527 24 8582  
E-mail: [info@dnw.aero](mailto:info@dnw.aero)



NWB  
Lilienthalplatz 7  
38108 Braunschweig  
Germany

Contact: A. Bergmann  
Phone: +49 531 295 2450  
Fax: +49 531 295 2829  
E-mail: [dnw-nwb@dnw.aero](mailto:dnw-nwb@dnw.aero)



TWG, HDG, KRG, RWG  
Bunsenstraße 10  
37073 Göttingen  
Germany

Contact: K.-W. Bock  
Phone: +49 551 709 2828  
Fax: +49 551 709 2888  
E-mail: [dnw-guk@dnw.aero](mailto:dnw-guk@dnw.aero)



KKK  
Linder Höhe  
51147 Köln  
Germany

Contact: R. Rebstock  
Phone: +49 2203 601 3700  
Fax: +49 2203 695 961  
E-mail: [dnw-kkk@dnw.aero](mailto:dnw-kkk@dnw.aero)



LLF, LST, ECF  
Voorsterweg 31  
8316 PR Marknesse  
The Netherlands

Contact: G.H. Hegen  
Phone: +31 527 24 8519  
Fax: +31 527 24 8582  
E-mail: [info@dnw.aero](mailto:info@dnw.aero)



---

German-Dutch Wind Tunnels